LHCb-note 2007-054

24 Jan 2008

LHCb's Potential to Measure Flavour-Specific CP-Asymmetry in Semileptonic and Hadronic B_s^0 Decays

Nick Brook[1], Noel Cottingham[1], Robert W. Lambert[2], Franz Muheim[2], Jonas Rademacker[1], Paul Szczypka[1], Yuehong Xie[2]

[1] H. H. Wills Physics Lab, University of Bristol, Tyndall Avenue, Bristol BS8 1TL, UK
[2] School of Physics, University of Edinburgh, Mayfield Road, Edinburgh EH9 3JZ, UK

Abstract

The CP asymmetry in $\mathrm{B_s^0} - \overline{\mathrm{B}}{}_\mathrm{s}^0$ mixing, denoted as a^s_{fs}, is sensitive to new weak phases in the presence of physics beyond the Standard Model. This can be probed through a measurement of the time-dependent charge asymmetry $A^s_{fs}(t)$ in flavour-specific decays. This note describes the LHCb strategy to measure a^s_{fs} using a time-dependent method, in flavour untagged decays of $\mathrm{B_s^0} \to \mathrm{D_s^-}\mu^+\nu_\mu$ and $\mathrm{B_s^0} \to \mathrm{D_s^-}\pi^+$. We also investigate a measurement of the difference of a^s_{fs} and a^d_{fs} in $\mathrm{B_s^0} \to \mathrm{D_s^-}\mu^+\nu_\mu$ and $\mathrm{B_d^0} \to \mathrm{D^-}\mu^+\nu_\mu$ decays which allows to control the systematic uncertainty that arise from detection asymmetries.

Contents

1 Introduction

The CP violation in the B_s^0–$\overline{B}_s^0$ mixing is expected to be tiny in the Standard Model, but can be significantly enhanced in the presence of new CP-violating phases in general physics models [1]. This can be probed through measurement of the charge asymmetry in untagged flavour-specific decays such as $\overline{(B)}{}_s^0 \to D_s^{\pm}\mu^{\mp}\nu_\mu$ or $\overline{(B)}{}_s^0 \to D_s^{\pm}\pi^{\mp}$ [2]:

$$A_{fs}^s(t) = \frac{\Gamma(\overline{(B)}{}_s^0(t) \to f) - \Gamma(\overline{(B)}{}_s^0(t) \to \bar{f})}{\Gamma(\overline{(B)}{}_s^0(t) \to f) + \Gamma(\overline{(B)}{}_s^0(t) \to \bar{f})} \tag{1}$$

with $f = D_s^-\mu^+\nu_\mu$ or $D_s^-\pi^+$ and $\bar{f} = D_s^+\mu^-\bar{\nu}_\mu$ or $D_s^+\pi^-$. In our notation $A_{fs}^s(t)$ refers to the untagged time-dependent asymmetry which is different from the physical constant a_{fs}^s, which we aim to measure and will define later. If a_{fs}^s is measured in the semileptonic channel, it is sometimes also called a_{SL}^s or A_{SL}^s as in [2].

The LHCb experiment is expected to collect about 1 million $B_s^0 \to D_s^-\mu^+\nu_\mu$[1] events in $2\,\text{fb}^{-1}$ of data with a background to signal ratio of 0.36 [3], and 140 k $B_s^0 \to D_s^-\pi^+$ events in $2\,\text{fb}^{-1}$ of data with a background to signal ratio of 0.4 [4]. These huge event samples will provide an opportunity to measure A_{fs}^s with a high statistical precision.

The measured untagged time-dependent asymmetry $A_{fs}^s(t)$ depends on three parameters, a_{fs}, the production asymmetry and the charge detection asymmetry. Two of them can be extracted simultaneously, while the third has to be taken from other measurements. In section 5.1 we present the results of the Monte Carlo study of a simultaneous measurement of a_{fs}^s and the production asymmetry, assuming the detection asymmetry can be obtained from elsewhere. Besides the important measurement of a_{fs}^s itself, the measurement of the production asymmetry provides valuable input to many other analyses.

In section 6.3 we present a technique for measuring CP violation in B mixing that removes the need for external input on the detection asymmetry, using a simultaneous analysis of the time-dependent asymmetry in the B_s^0 system, $A_{fs}^s(t)$ and the equivalent quantity in the B_d^0 system:

$$A_{fs}^d(t) = \frac{\Gamma(\overline{(B)}{}^0(t) \to f) - \Gamma(\overline{(B)}{}^0(t) \to \bar{f})}{\Gamma(\overline{(B)}{}^0(t) \to f) + \Gamma(\overline{(B)}{}^0(t) \to \bar{f})}. \tag{2}$$

where both the B_d^0 and the B_s^0 decay to the same final state. This technique measures the difference of the CP-violation parameter a_{fs}^s in the B_s^0 system and the equivalent parameter in the B_d^0 system, a_{fs}^d. This combination of parameters, $a_{fs}^s - a_{fs}^d$, is interesting, and sensitive to New Physics by itself. Using results for a_{fs}^d from the B_d^0 factories [5, 6], a_{fs}^s can be extracted.

This note is organised as follows. Section 2 gives a brief description of the theory of B_s^0 mixing, the methods to extract a_{fs}^s in flavour specific decays, the prediction of a_{fs}^s in the Standard Model and the effect of new physics on a_{fs}^s. Section 4 summarises the current

[1] Here, and in the rest of this note, this notation always implies charged-conjugate modes with and without oscillation, unless the context requires otherwise. So the combined expected yield of $B_s^0 \to D_s^-\mu^+\nu_\mu$, $B_s^0 \to D_s^+\mu^-\bar{\nu}_\mu$, $\overline{B}_s \to D_s^-\mu^+\nu_\mu$, $\overline{B}_s \to D_s^+\mu^-\bar{\nu}_\mu$ is 1M in $2\,\text{fb}^{-1}$.

measurements of a^s_{fs}. The fast Monte Carlo simulation method for assessing statistical precision and results are presented in Section 5. Section 6 discusses an alternative strategy to measure a^s_{fs}. We conclude in Section 7.

2 Theory

In the following we summarise the relevant parameters involved in neutral B^0 mixing and in particular a time-dependent a_{fs} measurement, where we first describe the theory and then take into account detector effects. In our description of the B^0 mixing and decay formalism we follow references [2,7,8]. This short summary applies generically to systems of neutral B mesons. Where we refer to specific system, i.e. B^0_d or B^0_s, we add a subscript as in $\Delta\Gamma_d$, $\Delta\Gamma_s$ or a superscript as in a^d_{fs}, a^s_{fs}. The generic subscript/superscript q, such as $\Delta\Gamma_q$ or a^q_{fs} is used when we refer to both systems at the same time.

2.1 Mixing Parameters $\Delta\Gamma, \Delta m, a_{fs}$

The Schrödinger Equation for a superposition of flavour eigenstates, $a|\mathrm{B}^0\rangle + b|\overline{\mathrm{B}}^0\rangle$, is:

$$i\frac{\mathrm{d}}{\mathrm{d}t}\begin{pmatrix} a \\ b \end{pmatrix} = \mathbf{H}\begin{pmatrix} a \\ b \end{pmatrix}. \tag{3}$$

This is the Schrödinger Equation restricted to the $|\mathrm{B}^0\rangle - |\overline{\mathrm{B}}^0\rangle$ subspace of state vectors. The system is allowed to leave the $|\mathrm{B}^0\rangle - |\overline{\mathrm{B}}^0\rangle$ subspace by decaying to other particles, hence $\mathbf{H}$ in equation 3 will not be Hermitian. A general matrix $\mathbf{H}$ can be expressed in term of the Hermitian matrices $\mathbf{M}$ and $\mathbf{\Gamma}$ as

$$\mathbf{H} = \mathbf{M} - \frac{i}{2}\mathbf{\Gamma} \tag{4}$$

where the Hermitian part $\mathbf{M}$ represents the energy (mass) of the system, while the non-Hermitian part $\frac{i}{2}\mathbf{\Gamma}$ the decay to other states. $\mathcal{CPT}$ invariance implies

$$\langle \mathrm{B}^0|\mathbf{H}|\mathrm{B}^0\rangle = \langle \overline{\mathrm{B}}^0|\mathbf{H}|\overline{\mathrm{B}}^0\rangle. \tag{5}$$

Therefore the diagonal elements of $\mathbf{H}$ are the same and $\mathbf{H}$ can be written as:

$$\mathbf{H} = \begin{pmatrix} h_{11} & h_{12} \\ h_{21} & h_{11} \end{pmatrix}. \quad \text{with} \quad \mathbf{M} = \begin{pmatrix} M_{11} & M_{12} \\ M^*_{12} & M_{11} \end{pmatrix}, \ \mathbf{\Gamma} = \begin{pmatrix} \Gamma_{11} & \Gamma_{12} \\ \Gamma^*_{12} & \Gamma_{11} \end{pmatrix}. \tag{6}$$

The physical meson states with well-defined mass and decay width are the eigenvectors of $\mathbf{H}$:

$$|B_{H,L}\rangle = p|\mathrm{B}^0\rangle \mp q|\overline{\mathrm{B}}^0\rangle \tag{7}$$

The subscripts L and H stand for the "light" and the "heavy" physical B^0-states, which have masses $M_{H,L}$ and widths $\Gamma_{H,L}$. The mass- and width difference between those states is:

$$\Delta m = M_H - M_L, \quad \Delta\Gamma = \Gamma_L - \Gamma_H \tag{8}$$

The average B^0 lifetime is

$$\Gamma \equiv \frac{1}{2}\left(\Gamma_L + \Gamma_H\right) \tag{9}$$

It is useful to define the following quantity:

$$\phi \equiv \arg(-M_{12}/\Gamma_{12}) \tag{10}$$

The mass and width difference in the B^0 system are related to M_{ij}, Γ_{ij} by:

$$\begin{aligned} (\Delta m)^2 - \frac{1}{4}(\Delta\Gamma)^2 &= 4\left|M_{12}\right|^2 - \left|\Gamma_{12}\right|^2, \\ \Delta m \Delta\Gamma &= 4\mathsf{Re}(M_{12}\Gamma_{12}^*) = 4\left|M_{12}\Gamma_{12}\right|\cos\phi \end{aligned} \tag{11}$$

To a good approximation for the B_s^0 and B_d^0 system [8]:

$$\Delta m = 2\left|M_{12}\right| \quad \Delta\Gamma = 2\left|\Gamma_{12}\right|\cos\phi \tag{12}$$

Equation 11 or 12 link two observables $(\Delta\Gamma, \Delta m)$ to three parameters, $\left|M_{12}\right|, \left|\Gamma_{12}\right|, \phi$. A third observable, allowing to solve the system, is

$$a_{fs} \equiv \mathsf{Im}\frac{\Gamma_{12}}{M_{12}} = \frac{\Delta\Gamma}{\Delta m}\tan\phi \tag{13}$$

The subscript fs stands for "flavour-specific", since it is measured in flavour-specific decays (see below). Usually these are semileptonic decays, and therefore it is often referred to as a_{sl}. This parameter is related to p, q by:

$$1 - \left|\frac{q}{p}\right| = \frac{a_{fs}}{2} \tag{14}$$

Thus it measures a deviation of $\left|\frac{q}{p}\right|$ from unity and hence CP violation in the mixing of the B and $\bar{B}$ mesons. In the Standard Model this is expected to be a very small effect.

2.2 a_{fs}^q in the Standard Model

M_{12}^q and Γ_{12}^q are predicted in the Standard Model (SM) and related to other CKM parameters [9]:

$$M_{12}^q = -\frac{G_F^2 m_w^2 \eta_B m_{B_q} B_{B_q} f_{B_q}^2}{12\pi^2} S_o\left(\frac{m_t^2}{m_W^2}\right)(V_{tq}^* V_{tb})^2 \tag{15}$$

$$\Gamma_{12}^q = \frac{G_F^2 m_b^2 \eta_B' m_{B_q} B_{B_q} f_{B_q}^2}{8\pi^2}\left[(V_{tq}^* V_{tb})^2 + V_{tq}^* V_{tb} V_{cq}^* V_{cb}\mathcal{O}\left(\frac{m_c^2}{m_b^2}\right) + (V_{cq}^* V_{cb})^2\mathcal{O}\left(\frac{m_c^2}{m_b^2}\right)\right] \tag{16}$$

where G_F is the Fermi constant, m_W the W boson mass, and m_i the mass of quark i; m_{B_q}, f_{B_q} and B_{B_q} are the B_q^0 mass, decay constant and bag parameter, respectively. $S_0(x_t)$ is

a known Inami-Lin function approximated very well by 0.784 $x_t^{0.76}$, V_{ij} are the elements of the CKM matrix, η_B and η'_B are QCD corrections of order unity.

Within the SM a^q_{fs} is small [10], but non-zero, as (c.f. equation 13):

$$\left|\frac{\Gamma^q_{12}}{M^q_{12}}\right| = \mathcal{O}\left(\frac{m_b^2}{m_t^2}\right) \ll 1 \tag{17}$$

$$\arg\left(-\frac{\Gamma^q_{12}}{M^q_{12}}\right) = \mathcal{O}\left(\frac{m_c^2}{m_b^2}\right) \ll 1 \tag{18}$$

$$a^q_{fs} \propto -\mathsf{Im}\left(\frac{V^*_{cq}V_{cb}}{V^*_{tq}V_{tb}}\right) \tag{19}$$

Including next-to-leading order QCD corrections, using an operator basis reducing α_s and $1/m_b$ errors, [2] [11],

$$a^d_{fs} = -(4.8^{+1.0}_{-1.2}) \times 10^{-4} \tag{20}$$

$$a^s_{fs} = +(2.06 \pm 0.57) \times 10^{-5} \tag{21}$$

Constraints on a^d_{fs} appear in the CKM unitarity triangle (UT) as circles of certainty/uncertainty touching the point ($\bar{\rho}$,$\bar{\eta}$) = (1,0) [10] [12], hence constraining the vertex of the UT.

2.3 a^q_{fs} with new physics

Precision flavour physics can illuminate/constrain wide avenues of possible new physics. In many new models significant departures from the SM are predicted for a^q_{fs} [13,14] with up to two orders of magnitude enhancement in the B^0_s system [1]. Much of the parameter space of new physics models has already been explored, however it is difficult to constrain models whose physics differs only slightly from the SM at LEP and LHC energies.

However, [15] and [10] find knowledge of the flavour-specific asymmetry can constrain new physics (NP) models even if :

1. They have no new flavour structure
2. They maintain a unitary CKM matrix
3. Tree level NP processes are SM dominated
4. They have no new CPV from direct or interference terms

The most general model-independent form parameterising NP in $B^0_{d,s}$ mixing is as follows, adopting the notations used in [1], [11] and [15]:

$$(\Gamma^q_{12})^{NP} = (\Gamma^q_{12})^{SM} \tag{22}$$

$$(M^q_{12})^{NP} = \Delta_q \cdot (M^q_{12})^{SM} = r_q^2 e^{2i\theta_q} (M^s_{12})^{SM} = \left(1 + h_q e^{2i\sigma_q}\right)(M^q_{12})^{SM} \tag{23}$$

where r_q^2 and h_q are real parameters representing the magnitude of new physics, σ_q and θ_q are real angles representing the phase of new physics and Δ_q is a complex parameter

encompassing information on the real and imaginary new physics contribution. These relations lead to:

$$(\Delta m_s)^{NP} = (\Delta m_s)^{SM} r_s^2 \tag{24}$$

$$(\Delta\Gamma_s)^{NP}_{CP} = (\Delta\Gamma_s)^{NP}\cos(2\theta_s) = (\Delta\Gamma_s)^{SM}\cos^2(2\theta_s) \tag{25}$$

$$\left(a^s_{fs}\right)^{NP} = \mathsf{Im}\left(\frac{\Gamma^s_{12}}{M^s_{12}}\right)^{SM}\frac{\cos(2\theta_s)}{r_s^2} - \mathsf{Re}\left(\frac{\Gamma^s_{12}}{M^s_{12}}\right)^{SM}\frac{\sin(2\theta_s)}{r_s^2} \tag{26}$$

where $(\Delta\Gamma_s)^{NP}_{CP}$ is the observable width difference between decays to CP-odd and CP-even states. The other new physics parameters can be derived geometrically using equation 23.

There are three necessary conditions in order that a measurement of the flavour specific asymmetry a^s_{fs} should constrain $2\theta_s$ [15]:

1. The experimental error on a^s_{fs} should be at or below $|\Gamma^s_{12}/M^s_{12}|^{SM}$
2. An upper bound on r_s^2 should be available
3. An independent upper bound on a^d_{fs} should be available

Reference [15] uses the $A^{s,d}_{SL}$ from present data given in section 4, and the Δm_s value from the CDF collaboration [16] to constrain $2\theta_s$:

$$\Delta m_s = (17.33^{+0.42}_{-0.21} \pm 0.07)\ \text{ps} \tag{27}$$

$$r_s^2 = \frac{\Delta m_s^{expt}}{\Delta m_s^{SM}} = (0.97 \pm 0.26) \tag{28}$$

$$\sin(2\theta_s) = -\frac{A^s_{SL}}{[\mathsf{Re}(\Gamma^s_{12}/M^s_{12})]^{SM}}\frac{\Delta m_s^{expt}}{\Delta m_s^{SM}} = -(1.9 \pm 2.8) \tag{29}$$

which is the limit assuming NP-dominance in A^s_{SL}. Constraints on new physics are indicated in Figures 1 ,2 and 3, with the experimental values discussed in Section 4. Reference [11] concludes: *"The current experimental situation shows a small deviation, which may become significant, if the experimental uncertainties in $\Delta\Gamma_s$, $a^s_{\rm sl}$ and ϕ_s will go down in near future."*

3 Measuring a_{fs}

In this section we develop the formalism measuring a_{fs} in untagged, time-dependent decay rate asymmetries in decays to flavour eigenstates, following closely [2, 7, 8]. An overview of the notation used in this section is given in appendix A.

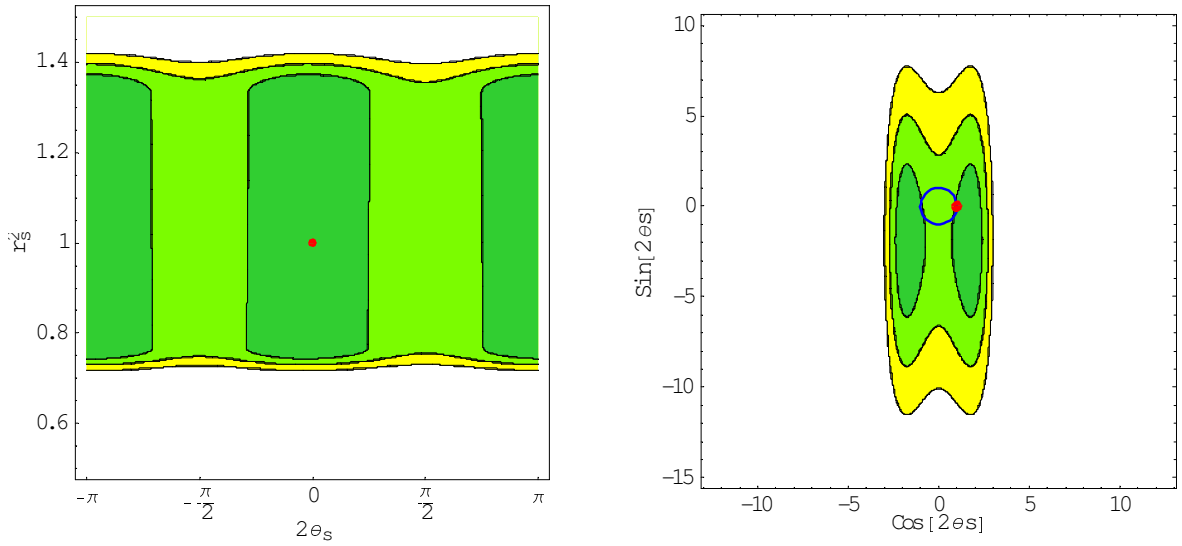

Figure 1: Constraints on NP from current data allowing for new physics in all loop processes. Left, In the $r_s^2 - 2\theta_s$ plane. Right in the $\cos(2\theta_s) - \sin(2\theta_s)$ plane. The dark green, light green and yellow regions correspond to probability higher than 0.32, 0.046, and 0.0027, respectively. The SM point, $2\theta_s = 0$, $r_s^2 = 1$, is marked with the solid red dot. Both Figures have been taken from [15].

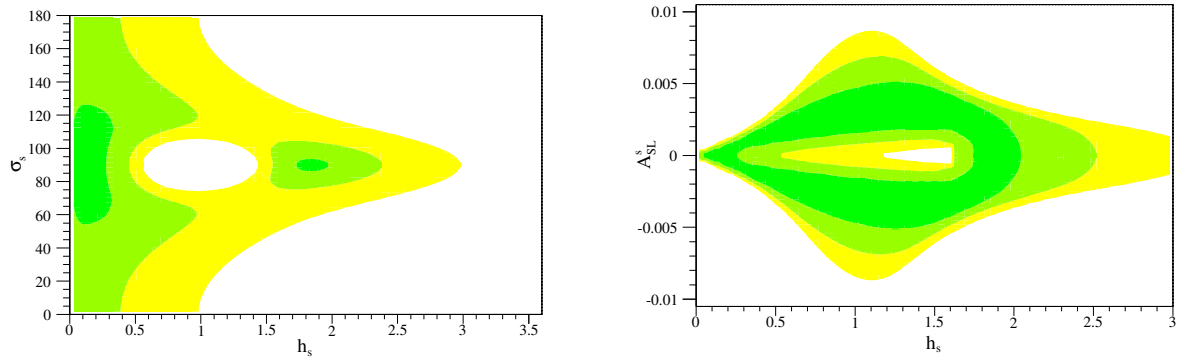

Figure 2: Constraints on NP from current data. Left, In the h_s, σ_s plane. Right indicating also the allowed A_{SL}^s as a function of h_s. The dark, medium, and light shaded areas have CL > 0.90, 0.32, and 0.05, respectively. The SM region is $h_s = 0$, σ_s undefined. Both Figures have been taken from [1].

3.1 Decay Rates

3.1.1 Decay Rates without Detector Effects

The time evolution of a B^0 that is a flavour eigenstate at $t = 0$ is given by:

$$\begin{aligned} |B^0(t)\rangle &= \frac{1}{2p}\left(e^{-(iM_L+\frac{1}{2}\Gamma_L)t}|B_L\rangle + e^{-(iM_H+\frac{1}{2}\Gamma_H)t}|B_H\rangle\right) \\ |\overline{B}^0(t)\rangle &= \frac{1}{2q}\left(e^{-(iM_L+\frac{1}{2}\Gamma_L)t}|B_L\rangle - e^{-(iM_H+\frac{1}{2}\Gamma_H)t}|B_H\rangle\right) \end{aligned} \quad (30)$$

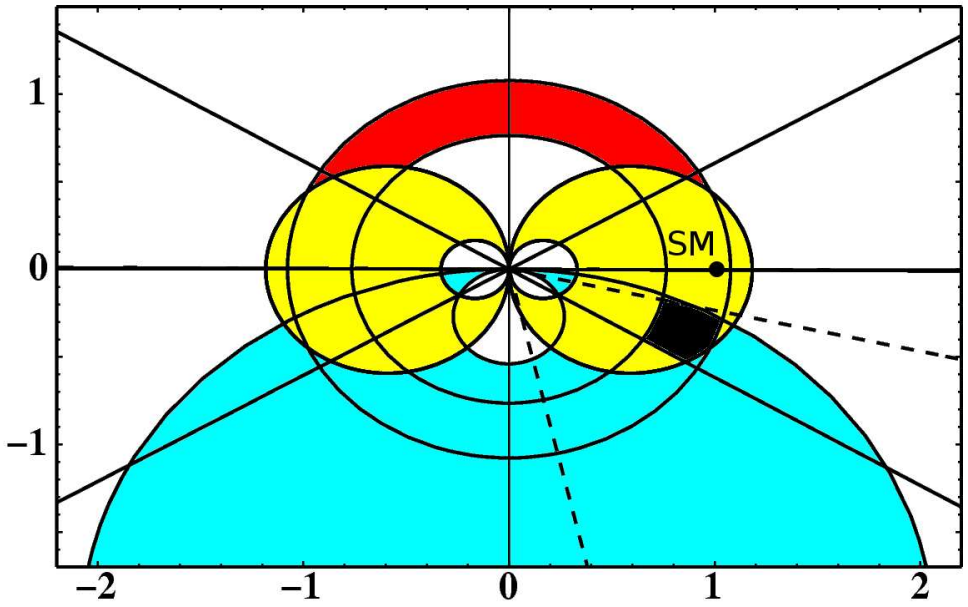

Figure 3: Constraints on NP from current data in the complex Δ_s-plane. The bound from ΔM_s is given by the red (dark-grey) annulus around the origin. The bound from $|\Delta\Gamma_s|/\Delta M_s$ is given by the yellow (light-grey) region and the bound from $a^s_{\rm fs}$ is given by the light-blue (grey) region. The solid lines are an extraction of the angle ϕ_s^Δ from $|\Delta\Gamma_s|$ with a four–fold ambiguity and the dashed line ϕ_s^Δ from the angular analysis in $B_s \to J/\Psi\phi$. The SM point, $\Delta_s = 1$, is marked with the solid dot. This Figure has been taken from [11].

where $|\mathrm{B}^0(t)\rangle$ is an oscillating B meson that was a B^0 at time $t = 0$, and $|\overline{\mathrm{B}}^0(t)\rangle$ a B-meson that was a $\overline{\mathrm{B}}^0$ at $t = 0$. In terms of flavour eigenstates:

$$\begin{array}{rcrcl} |\mathrm{B}^0(t)\rangle & = & g_+(t)|\mathrm{B}^0\rangle & + & \frac{q}{p}\; g_-(t)|\overline{\mathrm{B}}^0\rangle \\ |\overline{\mathrm{B}}^0(t)\rangle & = & \frac{p}{q}\; g_-(t)|\mathrm{B}^0\rangle & + & g_+(t)|\overline{\mathrm{B}}^0\rangle \end{array} \tag{31}$$

with

$$\begin{aligned} g_+(t) &= e^{-im\,t-\frac{1}{2}\Gamma\,t}\left\{\cosh\left(\frac{1}{4}\Delta\Gamma\,t\right)\cos\left(\frac{1}{2}\Delta m\,t\right) - i\sinh\left(\frac{1}{4}\Gamma\,t\right)\sin\left(\frac{1}{2}\Delta m\,t\right)\right\} \\ g_-(t) &= e^{-im\,t-\frac{1}{2}\Gamma\,t}\left\{-\sinh\left(\frac{1}{4}\Delta\Gamma\,t\right)\cos\left(\frac{1}{2}\Delta m\,t\right) + i\cosh\left(\frac{1}{4}\Gamma\,t\right)\sin\left(\frac{1}{2}\Delta m\,t\right)\right\} \end{aligned} \tag{32}$$

Denoting the decay amplitude of a B^0-flavour eigenstate to a final state f with $\langle f|H_I|\mathrm{B}^0\rangle = A_f$ (H_I represents the interaction Hamiltonian) and of a $\overline{\mathrm{B}}^0$ to $\bar{f}$ with $\bar{A}_{\bar{f}}$, etc, decays to

flavour eigenstates are characterised by $A_{\bar{f}} = \bar{A}_f = 0$. For such decays:

$$\Gamma\left(\mathrm{B}^0 \to f\right)(t) = N_f |A_f|^2 |g_+|^2 \tag{33}$$

$$\Gamma\left(\mathrm{B}^0 \to \bar{f}\right)(t) = \left|\frac{q}{p}\right|^2 N_f |\bar{A}_{\bar{f}}|^2 |g_-|^2 \tag{34}$$

$$\Gamma\left(\overline{\mathrm{B}}^0 \to \bar{f}\right)(t) = N_f |\bar{A}_{\bar{f}}|^2 |g_+|^2 \tag{35}$$

$$\Gamma\left(\overline{\mathrm{B}}^0 \to f\right)(t) = \left|\frac{p}{q}\right|^2 N_f |A_f|^2 |g_-|^2 \tag{36}$$

where N_f is a normalisation factor which is identical for all 4 decay rates. For the next step we use:

$$\begin{aligned} \left|\frac{q}{p}\right|^2 &= \left(1 - \frac{a_{fs}}{2}\right)^2 = 1 - a_{fs} + \mathcal{O}\left(a_{fs}^2\right) \\ \left|\frac{p}{q}\right|^2 &= \frac{1}{\left(1 - \frac{a_{fs}}{2}\right)^2} = 1 + a_{fs} + \mathcal{O}\left(a_{fs}^2\right) \end{aligned} \tag{37}$$

Replacing $\left|\frac{q}{p}\right|^2$ and $\left|\frac{p}{q}\right|^2$ with the first-order expressions in a_{fs}, and writing out $|g_\pm|^2$, we find:

$$\Gamma\left(\mathrm{B}^0 \to f\right)(t) = N_f |A_f|^2 e^{-\Gamma t} \frac{1}{2} \left\{ \cosh\left(\frac{1}{2}\Delta\Gamma\, t\right) + \cos\left(\Delta m\, t\right) \right\} \tag{38}$$

$$\Gamma\left(\mathrm{B}^0 \to \bar{f}\right)(t) = N_f \left(1 - a_{fs}\right) \left|\bar{A}_{\bar{f}}\right|^2 e^{-\Gamma t} \frac{1}{2} \left\{ \cosh\left(\frac{1}{2}\Delta\Gamma\, t\right) - \cos\left(\Delta m\, t\right) \right\} \tag{39}$$

$$\Gamma\left(\overline{\mathrm{B}}^0 \to \bar{f}\right)(t) = N_f \left|\bar{A}_{\bar{f}}\right|^2 e^{-\Gamma t} \frac{1}{2} \left\{ \cosh\left(\frac{1}{2}\Delta\Gamma\, t\right) + \cos\left(\Delta m\, t\right) \right\} \tag{40}$$

$$\Gamma\left(\overline{\mathrm{B}}^0 \to f\right)(t) = N_f \left(1 + a_{fs}\right) |A_f|^2 e^{-\Gamma t} \frac{1}{2} \left\{ \cosh\left(\frac{1}{2}\Delta\Gamma\, t\right) - \cos\left(\Delta m\, t\right) \right\} \tag{41}$$

3.1.2 Finite Time Resolution

To obtain the measured decay rates with finite time resolution we need to convolve the expression 38 - 41 with an appropriate resolution function, here we choose a Gaussian (more complicated models can be obtained easily from this by adding up Gaussians of different width). The decay rates as a function of the measured time t are therefore obtained by solving:

$$\Gamma_j(t) = f_j(a_{fs}) \int_0^\infty e^{-\Gamma t'} \left(\cosh\left(\frac{1}{2}\Delta\Gamma\, t'\right) \pm \cos\left(\Delta m\, t'\right) \right) \frac{1}{\sqrt{2\pi}\sigma} e^{\frac{(t'-t)^2}{2\sigma^2}} dt' \tag{42}$$

where the index j labels the four decay rates given in Equations 38 - 41, and f_j is a time-independent parameter that is different for each of the four decay modes. The details of

the calculations are given in Appendix B. The result is:

$$\begin{aligned}\Gamma_j(t) = \quad & f_j(a_{fs})e^{-\Gamma t}\, e^{\frac{1}{2}\Gamma^2\sigma^2}\left[e^{\frac{1}{8}\sigma^2(\Delta\Gamma)^2}\left\{\right.\right. \\ & \frac{1}{2}\, e^{\frac{1}{2}\Delta\Gamma\left(t-\sigma^2\Gamma\right)}\mathrm{Freq}\left(\frac{t}{\sigma}-\sigma\left(\Gamma-\frac{1}{2}\Delta\Gamma\right)\right) \\ + \quad & \left.\left.\frac{1}{2}\, e^{-\frac{1}{2}\Delta\Gamma\left(t-\sigma^2\Gamma\right)}\mathrm{Freq}\left(\frac{t}{\sigma}-\sigma\left(\Gamma+\frac{1}{2}\Delta\Gamma\right)\right)\right\} \\ \pm \quad & e^{-\frac{1}{2}\Delta m^2\sigma^2}\mathsf{Re}\left\{e^{i\Delta m\left(t-\Gamma\sigma^2\right)}\right. \\ & \left.\left.\times\left(\frac{1}{2}-i\frac{1}{2}\mathrm{erfi}\left(\frac{\Delta m\sigma+i\left(\frac{t}{\sigma}-\sigma\Gamma\right)}{\sqrt{2}}\right)\right)\right\}\right] \end{aligned} \tag{43}$$

where Freq is the frequency function, defined by

$$\mathrm{Freq}(y) \equiv \int_{-\infty}^{y} e^{-\frac{1}{2}x^2}\, dx \tag{44}$$

and erfi is the imaginary error function defined by:

$$\mathrm{erfi}(z) = -i\mathrm{erf}(iz) \tag{45}$$

Both functions can be calculated with standard algorithms, available for example in root (see Appendix B for details). The expression simplifies significantly if we assume that $t \gg \sigma$, because then the Freq(y) terms tend towards 1 and erfi(z) terms towards i.

$$\begin{aligned}&\Gamma_j(t) = \\ &\quad f_j(a_{fs})e^{-\Gamma t+\frac{1}{2}\Gamma^2\sigma^2}\left[e^{\frac{1}{8}\sigma^2(\Delta\Gamma)^2}\cosh\left(\frac{1}{2}\Delta\Gamma\left(t-\sigma^2\Gamma\right)\right)\pm e^{-\frac{1}{2}\Delta m^2\sigma^2}\cos\left(\Delta m\left(t-\Gamma\sigma^2\right)\right)\right] \\ &\quad \text{for } t \gg \sigma \end{aligned} \tag{46}$$

While it is perfectly possible to calculate the full expression 43 using the software referred to in Appendix B, for the purpose of this note we use the simpler expression 46 throughout. This is sufficiently accurate for decay times $t \geq 4\sigma$ (then Freq ≈ 1 and erfi $\approx i$ to a very good approximation). To ensure this assumption is valid we apply a minimum lifetime cut of $t > 5\sigma$. Since the data selection in all channels considered uses impact parameter cuts to select long-lived particles anyway, this additional cut has only a very small effect except for the set of toy MC experiments with the worst lifetime resolution. In the final data analysis one might have to use the full expression 43 to make best use of all available data, but for the purpose this study we believe these simplifications are acceptable.

3.2 Measuring a_{fs} with Untagged Decay Rates

Measuring a_{fs} requires decays to flavour-specific states. This means that, if the observed decays are $\mathrm{B}^0 \to \mathrm{f}$ and $\overline{\mathrm{B}}^0 \to \bar{\mathrm{f}}$, the direct decays $\mathrm{B}^0 \to \bar{\mathrm{f}}$ and $\overline{\mathrm{B}}^0 \to \mathrm{f}$ must be forbidden. Additionally, we require that there is no direct CP violation in the decay, i.e.:

$$|A_f| = \left|\bar{A}_{\bar{f}}\right| \tag{47}$$

where A_f is the amplitude for $\mathrm{B}^0 \to \mathrm{f}$ and $\bar{A}_{\bar{f}}$ the $\overline{\mathrm{B}}^0 \to \bar{\mathrm{f}}$ amplitude. Suitable decays are semileptonic B^0_d or B^0_s decays like $\mathrm{B}^0 \to \mathrm{X}\ell^+\nu_\ell$, as well as, in the B^0_s system, $\mathrm{B}^0_\mathrm{s} \to \mathrm{D}^+_\mathrm{s}\pi^-$ [2]. For such decays, a_{fs} can be extracted from the untagged decay rate asymmetry:

$$A_{fs}(t) = \frac{\Gamma(\mathrm{B}^0 \text{ or } \overline{\mathrm{B}}^0 \to f) - \Gamma(\mathrm{B}^0 \text{ or } \overline{\mathrm{B}}^0 \to \bar{f})}{\Gamma(\mathrm{B}^0 \text{ or } \overline{\mathrm{B}}^0 \to f) + \Gamma(\mathrm{B}^0 \text{ or } \overline{\mathrm{B}}^0 \to \bar{f})} \tag{48}$$

Note that acceptance effects (as long as they are charge-symmetric) cancel, which is of particular importance for hadronic decays at LHCb where the impact-parameter based trigger biases the lifetime distribution. If production rate for B^0 and $\overline{\mathrm{B}}^0$ are the same, and the detection efficiency of f is the same as that for $\bar{f}$, this is

$$A_{fs}(t) = \frac{\Big(\Gamma(\mathrm{B}^0 \to f) + \Gamma(\overline{\mathrm{B}}^0 \to f)\Big) - \Big(\Gamma(\overline{\mathrm{B}}^0 \to \bar{f}) + \Gamma(\mathrm{B}^0 \to \bar{f})\Big)}{\Big(\Gamma(\mathrm{B}^0 \to f) + \Gamma(\overline{\mathrm{B}}^0 \to f)\Big) + \Big(\Gamma(\overline{\mathrm{B}}^0 \to \bar{f}) + \Gamma(\mathrm{B}^0 \to \bar{f})\Big)} \tag{49}$$

where the rates Γ are those given in Equations 38 - 41, modified according to 46 to take into account finite time resolutions, leading to

$$A_{fs}(t) = \frac{a_{fs}}{2} \; - \; e^{-\frac{1}{2}\sigma^2\left((\Delta m)^2 + \left(\frac{1}{2}\Delta\Gamma\right)^2\right)} \left[\frac{a_{fs}}{2}\right] \frac{\cos\left(\Delta m \; (t - \sigma^2\Gamma)\right)}{\cosh\left(\frac{1}{2}\Delta\Gamma \, (t - \sigma^2\Gamma)\right)} \tag{50}$$

for the case that there is no production or detection asymmetry.

3.2.1 Production and Detection Asymmetry

At a $p-p$ collider, a production asymmetry between B^0 and $\overline{\mathrm{B}}^0$ mesons is to be expected. And any realistic detector is likely to have a detection asymmetry (charge asymmetry). Defining

- N rate of B^0 production, $\bar{N}$ rate of $\overline{\mathrm{B}}^0$ production
- ϵ_f detection efficiency for final state f, $\bar{\epsilon}_f$ detection efficiency for final state $\bar{f}$

the total, measured time-dependent asymmetry is given by

$$A_{fs}(t) = \frac{\Big(N\epsilon_f\Gamma(\mathrm{B}^0 \to f) + \bar{N}\epsilon_f\Gamma(\overline{\mathrm{B}}^0 \to f)\Big) - \Big(\bar{N}\bar{\epsilon}_f\Gamma(\overline{\mathrm{B}}^0 \to \bar{f}) + N\bar{\epsilon}_f\Gamma(\mathrm{B}^0 \to \bar{f})\Big)}{\Big(N\epsilon_f\Gamma(\mathrm{B}^0 \to f) + \bar{N}\epsilon_f\Gamma(\overline{\mathrm{B}}^0 \to f)\Big) + \Big(\bar{N}\bar{\epsilon}_f\Gamma(\overline{\mathrm{B}}^0 \to \bar{f}) + \bar{N}\bar{\epsilon}_f\Gamma(\mathrm{B}^0 \to \bar{f})\Big)} \tag{51}$$

It is useful make the following definitions:

$$\text{The production asymmetry:} \qquad A_p \equiv \frac{N-\bar{N}}{N+\bar{N}}. \tag{52}$$

$$\text{The detection asymmetry:} \qquad A_c \equiv \frac{\epsilon_f - \bar{\epsilon}_f}{\epsilon_f + \bar{\epsilon}_f}. \tag{53}$$

Equivalently one can define the following parameters, as in [2]:

$$\delta_p \equiv \frac{\bar{N}}{N} - 1 \qquad \delta_c \equiv \frac{\bar{\epsilon}_f}{\epsilon_f} - 1 \tag{54}$$

which are the deviations of the production and detection efficiency ratios from unity. These parameters are related to the production and detection asymmetries by

$$A_p = \frac{-\delta_p}{2+\delta_p}, \qquad \delta_p = \frac{-2A_p}{1+A_p} \tag{55}$$

$$A_c = \frac{-\delta_c}{2+\delta_c} \qquad \delta_c = \frac{-2A_c}{1+A_c} \tag{56}$$

In some cases it will be more convenient to use the "A" parameters and in others the "δ" parameters. Both are essentially equivalent, and to first order proportional to each other. For simplicity, we will often refer to either of them as "asymmetry" - which one is meant will be clear from the symbol used.

Further we define

$$\begin{aligned}
A'_p &\equiv -\tfrac{\delta_p+\frac{1}{2}\delta_p\delta_c}{2+\delta_p+\delta_c} = \tfrac{A_p}{1-A_pA_c} && \text{which is } \mathcal{O}(\delta)\\
A'_c &\equiv -\tfrac{\delta_c+\frac{1}{2}\delta_p\delta_c}{2+\delta_p+\delta_c} = \tfrac{A_c}{1-A_pA_c} && \text{which is } \mathcal{O}(\delta)\\
\delta A \equiv A'_p - A'_c &= -\tfrac{\delta_p-\delta_c}{2+\delta_p+\delta_c} = \tfrac{A_p-A_c}{1-A_pA_c} && \text{which is } \mathcal{O}(\delta)\\
D &\equiv \tfrac{\delta_p\delta_c}{2+\delta_p+\delta_c} = \tfrac{A_pA_c}{1-A_pA_c} && \text{which is } \mathcal{O}(\delta^2)
\end{aligned} \tag{57}$$

where we also indicate which order in the parameter $\delta \equiv \max(\delta_p, \delta_c)$ each expression is, and we assume that δ_c and δ_p are of similar magnitude. With these definitions we find the following relation for the time-dependent flavour-specific asymmetry $A_{fs}(t)$:

$$A_{fs}(t) = \frac{\frac{a_{fs}}{2} + A'_c - \left[\frac{a_{fs}}{2} - A'_p\right] e^{-\frac{1}{2}\sigma^2\left((\Delta m)^2+\left(\frac{1}{2}\Delta\Gamma\right)^2\right)} \frac{\cos\left(\Delta m\left(t-\sigma^2\Gamma\right)\right)}{\cosh\left(\frac{1}{2}\Delta\Gamma(t-\sigma^2\Gamma)\right)}}{1 + D - \delta A\frac{a_{fs}}{2} + \left[D + \delta A\frac{a_{fs}}{2}\right] e^{-\frac{1}{2}\sigma^2\left((\Delta m)^2+\left(\frac{1}{2}\Delta\Gamma\right)^2\right)} \frac{\cos(\Delta m\,(t-\sigma^2\Gamma))}{\cosh\left(\frac{1}{2}\Delta\Gamma(t-\sigma^2\Gamma)\right)}} \tag{58}$$

Neglecting all terms $\mathcal{O}\left(a_{fs}^2\right)$ and higher, as well as terms that contain at least one factor a_{fs} and one factor of $\mathcal{O}(\delta^2)$ and higher (e.g. $\mathcal{O}(a_{fs}\delta^2)$, $\mathcal{O}(a_{fs}\delta^3, \ldots)$) we find:

$$A_{fs}(t) = \frac{\left[\frac{a_{fs}}{2} + A_c\right] - \left[\frac{a_{fs}}{2} - A_p\right] e^{-\frac{1}{2}\sigma^2\left((\Delta m)^2+\left(\frac{1}{2}\Delta\Gamma\right)^2\right)} \frac{\cos\left(\Delta m\left(t-\sigma^2\Gamma\right)\right)}{\cosh\left(\frac{1}{2}\Delta\Gamma(t-\sigma^2\Gamma)\right)}}{1 + A_cA_p e^{-\frac{1}{2}\sigma^2\left((\Delta m)^2+\left(\frac{1}{2}\Delta\Gamma\right)^2\right)} \frac{\cos(\Delta m\,(t-\sigma^2\Gamma))}{\cosh\left(\frac{1}{2}\Delta\Gamma(t-\sigma^2\Gamma)\right)}} \tag{59}$$

If we also ignored terms $\mathcal{O}(\delta^2)$ and higher, in which case $A'_p \approx A_p \approx -\delta_p/2$ and $A'_c \approx A_c \approx -\delta_c/2$, we would recover the expression given in [2]. However, since we expect the production asymmetry to be $\mathcal{O}(\%)$, it is unlikely that $\delta^2 \ll a_{fs}$. For the case that there is no detection asymmetry, the above expression simplifies considerably:

$$A_{fs}(t) = \left[\frac{a_{fs}}{2}\right] - e^{-\frac{1}{2}\sigma^2\left((\Delta m)^2+\left(\frac{1}{2}\Delta\Gamma\right)^2\right)}\left[\frac{a_{fs}}{2} - A_p\right]\frac{\cos\left(\Delta m\ (t-\sigma^2\Gamma)\right)}{\cosh\left(\frac{1}{2}\Delta\Gamma\,(t-\sigma^2\Gamma)\right)} \quad \text{for } A_c = 0 \tag{60}$$

Similarly, for the case that there is no production asymmetry we get:

$$A_{fs}(t) = \left[\frac{a_{fs}}{2} + A_c\right] - e^{-\frac{1}{2}\sigma^2\left((\Delta m)^2+\left(\frac{1}{2}\Delta\Gamma\right)^2\right)}\left[\frac{a_{fs}}{2}\right]\frac{\cos\left(\Delta m\ (t-\sigma^2\Gamma)\right)}{\cosh\left(\frac{1}{2}\Delta\Gamma\,(t-\sigma^2\Gamma)\right)} \quad \text{for } A_p = 0 \tag{61}$$

So for a situation with no production asymmetry (e.g. an e^+e^- or a $p\bar{p}$ collider), one can in principle fit both at the same time the detection asymmetry and a_{fs}.

However, the LHC is a proton-proton collider with six valence quarks and zero valence antiquarks in the the initial state. Therefore different production rates of B^0 and $\bar{B}^0$ are expected. This leads to a non-zero production asymmetry, estimated to be of $\mathcal{O}(1\%)$ [17]. For the purpose of the MC study presented in Section 5.1, we assume $A_p = 1\%$ and that the detection asymmetry A_c is well known, and present the statistical uncertainty for a simultaneous fit to the production asymmetry and a_{fs}. For simplicity, we assume that $A_c = 0$. A strategy of extracting the detection asymmetry from simultaneous fits to A^d_{fs} and A^s_{fs} is discussed in Section 6.

4 Current Measurements of $A^{s,d}_{SL}$

The term semileptonic asymmetry, A_{SL}, is used to describe the measured charge asymmetry (usually time-integrated) in semileptonic b-decays. We use the terms A^q_{SL} as the flavour-specific asymmetries which are extracted through measurement of A_{SL} and are equivalent to a^q_{fs}. The semileptonic decay is flavour-specific due to the charged W-boson emission, whose charge is determined by the flavour of the b-quark. The BABAR [5], BELLE [6], CLEO [18], D0 [19] and CDF [20] experiments studied the di-lepton asymmetry, that is examining events where two b-mesons are produced of correlated flavour. Where both these mesons decay semileptonically to leptons with the same charge, one of the two mesons must have oscillated into its partner. For a $\mathrm{B^0_s}$ meson it likely oscillated several times.

At the $\Upsilon(4S)$ resonance, i.e. for the BABAR, BELLE and CLEO experiments, only pairs of $\mathrm{B^0_d}$-$\mathrm{\overline{B}^0_d}$ and $\mathrm{B^+}$-$\mathrm{B^-}$ mesons are produced. Events with two leptons (electrons or muons) of opposite or same charge are labelled Right-Sign (RS) and a Wrong-Sign (WS), respectively. Examining the time-integrated decay rates in the di-lepton sample (untagged), these experiments measure [5, 18]:

$$A^{\Upsilon(4S)}_{SL} = A^d_{SL} = \frac{\Gamma^{WS}_d\bar{\Gamma}^{RS}_d - \bar{\Gamma}^{WS}_d\Gamma^{RS}_d}{\Gamma^{WS}_d\bar{\Gamma}^{RS}_d + \bar{\Gamma}^{WS}_d\Gamma^{RS}_d} \approx A^d_{fs} \tag{62}$$

where we neglected direct CP violation in B^0_d decays, $\bar{\Gamma}^{RS}_d = \Gamma^{RS}_d$ [15]. The detection asymmetry is measured and corrected for. Calculating the naive average of BABAR, BELLE, and CLEO values [15] find:

$$A^d_{SL} = +(1.1 \pm 5.5) \times 10^{-3} \tag{63}$$

At the Tevatron, which is a $p\bar{p}$ collider, DØ and CDF examine the di-muon sample which contains a mixture of B^0_s and B^0_d decays and measure the time-integrated asymmetry of the rate of same charge muon pairs Γ^{++} and Γ^{--} [20, 23, 24]:

$$\begin{aligned}
\Gamma^{++} &= \Gamma(b\bar{b} \to \mu^+\mu^+ X) \\
\Gamma^{--} &= \Gamma(b\bar{b} \to \mu^-\mu^- X) \\
A^{TeV}_{SL} &= \frac{\Gamma^{++} - \Gamma^{--}}{\Gamma^{++} + \Gamma^{--}} && (64) \\
A^{D\emptyset}_{SL} &= -(9.2 \pm 4.4(stat) \pm 3.2(syst)) \times 10^{-3} \div \left[1 + \frac{f_s Z_s}{f_d Z_d}\right] && (65) \\
A^{CDF}_{SL} &= +(8.0 \pm 9.0(stat) \pm 6.8(syst)) \times 10^{-3} && (66)
\end{aligned}$$

Note that in Equation 65 the definition of $A^{D\emptyset}_{SL}$ differs by a scale factor from the standard one [2]. The A_{SL} measurements are related to $a^{s,d}_{fs}$ through:

$$\begin{aligned}
A^{TeV}_{SL} &= \frac{f^{TeV}_d Z^{TeV}_d a^d_{fs} + f^{TeV}_s Z^{TeV}_s a^s_{fs}}{f^{TeV}_d Z^{TeV}_d + f^{TeV}_s Z^{TeV}_s} \approx 0.6\, a^d_{fs} + 0.4\, a^s_{fs} && (67) \\
&[\, = (0.582 \pm 0.030) a^d_{fs} + (0.418 \pm 0.047) a^s_{fs} \quad] && (68)
\end{aligned}$$

These relations are a Standard Model prediction using the parameters f_q, the fraction of B^0_q in the sample, and Z_q, relating the mixing and decay times [15], which are determined experimentally [21, 22]. This makes use of an approximation taking the SU(3) limit–that the semileptonic widths of the B^0_d and B^0_s meson are equal $\Gamma^s_{SL} = \Gamma^d_{SL}$. Equation 68 is given by [11]. Using this approach to combine the measured A_{SL} values at the Tevatron with the average of A^d_{SL} from the B-factories allow to indirectly determine A^s_{fs} [20, 23] [3]:

$$\begin{aligned}
&\text{DØ-indirect:} \quad A^s_{SL} = -(6.4 \pm 10.1) \times 10^{-3} && (69) \\
&\text{CDF-indirect:} \quad A^s_{SL} = -(20 \pm 21(stat) \pm 16(syst) \pm 9(inputs)) \times 10^{-3} && (70)
\end{aligned}$$

or from [15] using an earlier DØ result with the naive B-factory average, Equation 63:

$$A^s_{SL} = -(8 \pm 11) \times 10^{-3} \tag{71}$$

Alternatively using the SM value for a^d_{fs} (Equation 20) one finds from [11]:

$$A^s_{SL} \mid_{a^d_{fs}} = -(5.2 \pm 3.9) \times 10^{-3} \tag{72}$$

[2] We thank Guennadi Borissov for explaining this feature of the D0 analysis.

[3] Different B-factory averages for A^d_{fs} have been used in Equations 69 to 72.

Recently DØ has also presented a time-integrated direct measurement of A^s_{SL} in the channel $B^0_s \to D^\pm_s \mu^\mp \nu_\mu$ [24]. They measure:

$$\text{DØ-direct:} \quad A^s_{SL} = \frac{N(\mu^+ \mathrm{D}_\mathrm{s}^-) - N(\mu^- \mathrm{D}_\mathrm{s}^+)}{N(\mu^+ \mathrm{D}_\mathrm{s}^-) + N(\mu^- \mathrm{D}_\mathrm{s}^+)} = A^s_{fs} \tag{73}$$

where $N(\mu^\pm \mathrm{D}_\mathrm{s}^\mp)$ is the number of time-integrated $\mathrm{B}^0_\mathrm{s} \to \mathrm{D}^\pm_\mathrm{s} \mu^\mp \nu_\mu$ decays. Here the detector asymmetry is again corrected.

This measurement has a relatively small systematic contributions, in comparison to the dilepton sample, however the total error is dominated by the statistical error. For 27K events recorded in $1.3\,\mathrm{fb}^{-1}$, with a B/S ~ 0.2, DØ obtain [23]:

$$\text{DØ-direct:} \quad A^s_{SL} = (2.45 \pm 1.93(\mathrm{stat}) \pm 0.35(\mathrm{syst})) \times 10^{-2} \tag{74}$$

5 Time-dependent Analysis

5.1 Monte Carlo Study

The time-dependent decay rates defined in equation 46 are created using standard Monte Carlo methods.

The detection efficiency vs lifetime at LHCb is biased against short lifetimes because LHCb's trigger selects events which have tracks with large impact parameters in order to select (long-lived) B mesons. To model this effect we use an acceptance function, ϵ, which takes the form:

$$\begin{aligned} \epsilon(t) &= \tfrac{(\beta(t-t_0))^3}{1+(\beta(t-t_0))^3} \quad \text{for } t \geq t_0 \\ \epsilon(t) &= 0 \qquad\qquad\qquad\quad \text{for } t < t_0 \end{aligned} \tag{75}$$

Figures 4 to 7 show example decay rate and asymmetry distributions for various settings. The distributions in figures 4 and 5 were created using a lifetime resolution of 36 fs. Figures 6 and 7 show the same distributions created using a poorer resolution (120 fs). It is worthwhile to note that increasing the lifetime resolution such that $\sigma \approx \frac{2\pi}{\Delta m}$ effectively "washes out" the oscillations, thereby decreasing our sensitivity to any parameter proportional to the cosine term in equation 60.

5.2 Sensitivity to a_{fs}

In our Monte Carlo studies we considered the following three scenarios:

- 815k $\mathrm{B}^0_s \to D^-_s \mu^+ \nu_\mu$ events with a lifetime resolution of 270 fs [3]
- 185k $\mathrm{B}^0_s \to D^-_s \mu^+ \nu_\mu$ events with a lifetime resolution of 120 fs [3] and
- 140k $\mathrm{B}^0_\mathrm{s} \to \mathrm{D_s}\pi$ events with a lifetime resolution of 36 fs [4].

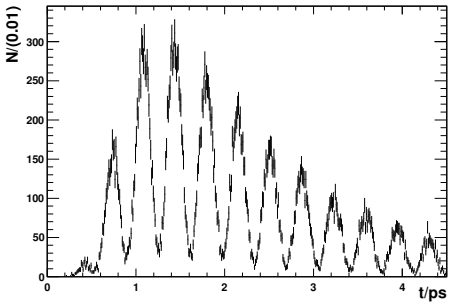

Figure 4: $B_s^0 \to D_s\pi$ decay distribution generated using the number of events expected in $2\,fb^{-1}$ and a lifetime resolution of 36 fs.

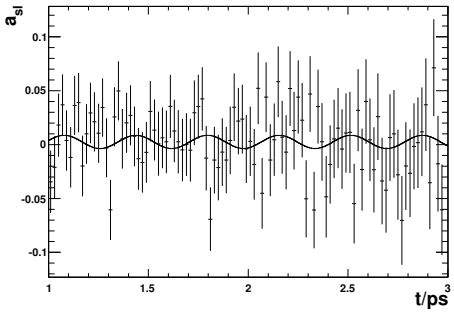

Figure 5: Generated asymmetry distribution for the $B_s \to D_s\pi$ channel with the theoretical prediction (smooth curve) superimposed. The lifetime resolution is 36 fs.

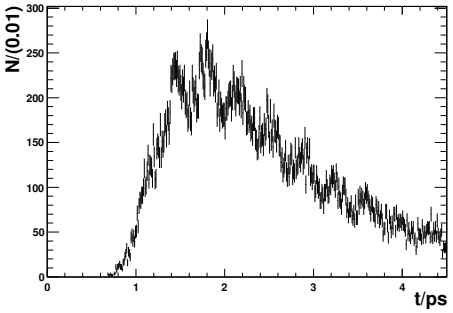

Figure 6: $B_s^0 \to D_s^-\mu^+\nu_\mu$ decay distribution generated using the number of events expected in $2\,fb^{-1}$ and a lifetime resolution of 120 fs.

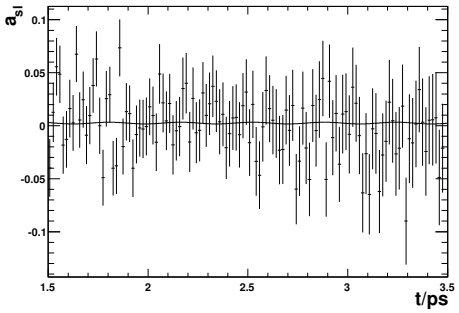

Figure 7: Generated asymmetry distribution for the $B_s^0 \to D_s^-\mu^+\nu_\mu$ channel with the theoretical prediction (smooth curve) superimposed. The lifetime resolution is 120 fs.

The differing lifetime resolutions in the two semi-leptonic scenarios is due to imposing a cut on the reconstructed invariant mass of the $D_s\mu$ combination. The lifetime resolution of events which pass the cut ($m(D_s\mu) > 4.5\,GeV$) is improved since less momentum is lost to the neutrino.

We investigated several parameter settings for each scenario [see table 3]. To test the validity of our study, we performed pull studies with at least 100 toy experiments each for each scenario and found the pull distributions to be consistent with a mean of zero and a width of one. Examples are given in figures 10 and 11 for scenario $B_s^0 \to D_s\mu\nu$.

From table 3 it can be seen that the measurement of the production asymmetry is highly dependent on the lifetime resolution. The precision on a_{fs} has no dependence on the time resolution, and for the case considered here, where $A_C = 0$, the time-independent part in the asymmetry (eqn. 60) ensures that we can fit a_{fs} even if the oscillations cannot be resolved at all. Both $\sigma_{a_{fs}}$ and σ_{A_p} are largely independent of the other input parameters and scale with $1/\sqrt{N}$.

Table 1 contains a summary of the obtained resolution per million events for each scenario and the corresponding resolutions when scaled to LHCb yields.

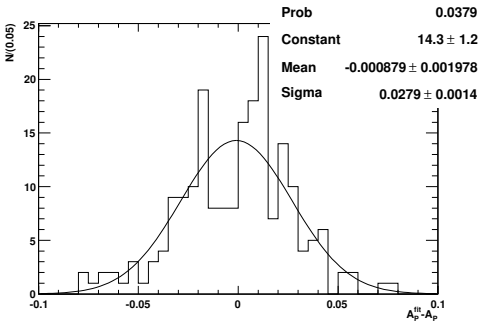

Figure 8: A_p resolution for the $\mathrm{B_s^0} \to \mathrm{D_s}\mu\nu(> 4.5$ GeV) scenario.

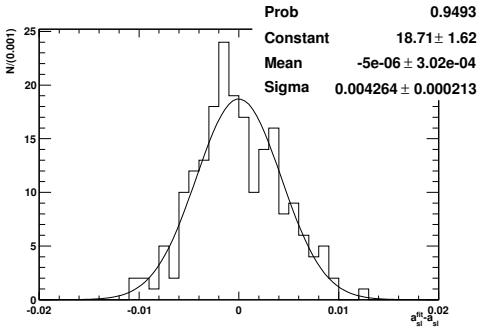

Figure 9: a_{fs} resolution for the $\mathrm{B_s^0} \to \mathrm{D_s}\mu\nu(> 4.5$ GeV) scenario.

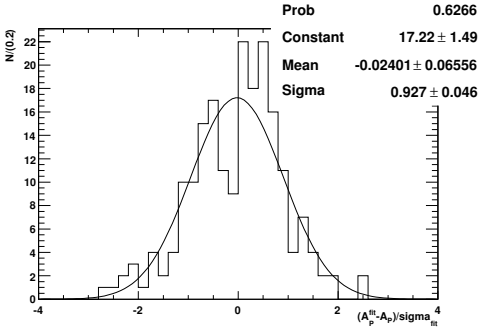

Figure 10: A_p pull distribution for the $\mathrm{B_s^0} \to \mathrm{D_s}\mu\nu(> 4.5$ GeV) scenario.

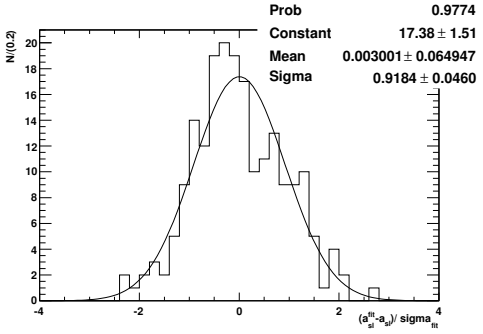

Figure 11: a_{fs} pull distribution for the $\mathrm{B_s^0} \to \mathrm{D_s}\mu\nu(> 4.5$ GeV) scenario.

Scenario $\mathrm{B_s^0} \to \ldots$	Resolution/ps	$\sigma_{a_{fs}}$/1M	$\sigma_{a_{fs}}/2\,\mathrm{fb}^{-1}$	σ_{A_p}/1M	$\sigma_{A_p}/2\,\mathrm{fb}^{-1}$
$D_s^-\mu^+\nu_\mu$ (< 4.5 GeV)	0.270	0.20%	0.22%	None	None
$D_s^-\mu^+\nu_\mu$ (> 4.5 GeV)	0.120	0.20%	0.47%	1.29%	3.01%
$\mathrm{D_s}\pi$	0.036	0.20%	0.53%	0.20%	0.53%

Table 1: a_{fs} and A_p resolution from selected scenarios after 1M events and $2\,fb^{-1}$ at LHCb respectively.

5.3 Non-Zero Charge Detection Asymmetry

Ignoring terms of order a_{fs}^2 and higher as well as $a_{fs}\delta^2$ and higher, as in equation 59 and used throughout this note, the time-independent part of the asymmetry is given by

$$A_{\mathsf{time-independent}} = \frac{a_{fs}}{2} + A_C \tag{76}$$

Scenario	resolution/ps	A_P Fit Result	a_{fs} Fit Result
$\mathrm{B_s^0} \to \mathrm{D_s}\mu\nu$	0.270	no resolution	$0.46\% \pm 0.22\%$
$\mathrm{B_s^0} \to \mathrm{D_s}\mu\nu$	0.120	$0.86\% \pm 3.01\%$	$0.54\% \pm 0.47\%$
$\mathrm{B_s^0} \to \mathrm{D_s}\pi$	0.030	$0.96\% \pm 0.53\%$	$0.52\% \pm 0.54\%$

Table 2: Effect of non-zero (but well-known) charge detection asymmetry on fit parameter resolution for the three physics scenarios. A_C was set to 2%.

and the only effect of a precisely known charge-detection aysmmetry is to add a constant to the measurement of a_{fs}. If we included higher order terms, we would also find that a non-zero A_C introduces a slight dependence of the time-independent part on A_P, but this effect is $\mathcal{O}(a_{fs}\delta^2)$, and can safely be ignored.

Table 2 shows results of fits of A_P and a^s_{fs} assuming a precisely known charge detection asymmetry of 2% for three Monte Carlo samples according to the three physics scenarios considered. The samples with good time resolution ($\sigma_\mathrm{t} = 36\,\mathrm{fs}$ and $\sigma_\mathrm{t} = 120\,\mathrm{fs}$) were fit without any constraint on A_P; in the fit to the sample with $\sigma_\mathrm{t} = 270\,\mathrm{fs}$ we constrained A_P to $1\% \pm 3\%$. We find that the resolutions on a_{fs} and A_P for $A_C = 2\%$ are compatible with those observed for $A_C = 0$.

5.4 Comparison to Tevatron Results

If systematic uncertainties can be controlled at a similar level, the LHCb result for $2\,\mathrm{fb}^{-1}$ of $\sigma_{a_{fs}} \sim 0.2\%$ will be a considerable improvement over the result we expect from DØ's direct measurement of a^s_{fs} by the end of Run II. Scaling their current statistical error to $6\,\mathrm{fb}^{-1}$, we expect $\sigma_{a^s_{fs}(D\emptyset-direct)} \sim 1\%$. Scaling the statistically more powerful indirect measurements at the Tevatron, which currently achieve a precision of better than 0.5% (see Sec 4), is more complicated because those measurements require outside input. Also, their systematic and statistical error are at a similar level.

For LHCb it is of course also the control of systematic uncertainties that is the main challenge in such a measurement, and DØ's analysis takes a lot of care to keep them low, including frequent switches of the magnetic field. How systematics could be controlled at LHCb using a simultaneous analysis of $\mathrm{B_s^0}$ and $\mathrm{B_d^0}$ decays is discussed in the following sections.

6 Measuring a_{fs} with $\mathrm{B}^0_s \to D^\pm_s \mu^\mp \nu_\mu$ and $\mathrm{B}^0_d \to D^\pm \mu^\mp \nu_\mu$ decays

In previous sections we have discussed time-dependent studies in the case where either the detection asymmetry is negligible or can be measured precisely in control channels elsewhere. In this section we consider the case where all the inherent asymmetries polluting the measurement are non-zero and/or measured to low precision, and discuss our strategies to limit or eliminate the resultant systematic errors.

These strategies are particularly important for the semileptonic channels, $B^0_s \to$

Dataset	resolution/ps	$\Delta\Gamma/ps^{-1}$	t_0/ps	N_{evts}	A_P	a_{fs}	A_P Fit Result $/10^{-2}$	a_{fs} Fit Result $/10^{-3}$
$B_s \to D_s \mu\nu$	0.270	0.071	1.50	815000	0.01	0.005	No resolution	5.05 ± 2.22
$B_s \to D_s \mu\nu$ ("Std setting")	0.120	0.071	0.60	185000	0.01	0.005	0.98 ± 3.01	5.12 ± 4.65
$B_s \to D_s \pi$	0.036	0.071	0.18	140000	0.01	0.005	1.07 ± 0.53	5.40 ± 5.35
$\text{Std}_{\Delta\Gamma=0\%\times\Gamma}$	0.120	0.000	0.60	185000	0.01	0.005	0.76 ± 2.99	6.91 ± 4.65
$\text{Std}_{\Delta\Gamma=5\%\times\Gamma}$	0.120	0.036	0.60	185000	0.01	0.005	1.18 ± 3.00	6.03 ± 4.65
$\text{Std}_{\Delta\Gamma=15\%\times\Gamma}$	0.120	0.107	0.60	185000	0.01	0.005	0.76 ± 3.03	6.59 ± 4.65
$\text{Std}_{\sigma=0\,fs}$	0.000	0.071	0.60	185000	0.01	0.005	0.99 ± 0.40	5.96 ± 4.65
$\text{Std}_{\sigma=60\,fs}$	0.060	0.071	0.60	185000	0.01	0.005	1.12 ± 0.62	6.48 ± 4.65
$\text{Std}_{\sigma=133\,fs}$	0.133	0.071	0.60	185000	0.01	0.005	1.12 ± 4.97	6.06 ± 4.65
$\text{Std}_{\sigma=320\,fs}$	0.320	0.071	1.60	185000	0.01	0.005	No resolution	8.51 ± 4.64
$\text{Std}_{a_{fs}=0.00}$	0.120	0.071	0.60	185000	0.01	0.000	0.87 ± 3.01	0.44 ± 4.65
$\text{Std}_{a_{fs}=0.01}$	0.120	0.071	0.60	185000	0.01	0.001	0.71 ± 3.01	2.89 ± 4.65
$\text{Std}_{a_{fs}=0.05}$	0.120	0.071	0.60	185000	0.01	0.005	0.98 ± 3.01	5.12 ± 4.65
$\text{Std}_{a_{fs}=0.10}$	0.120	0.071	0.60	185000	0.01	0.010	1.03 ± 3.01	12.4 ± 4.65
$\text{Std}_{a_{fs}=0.15}$	0.120	0.071	0.60	185000	0.01	0.015	0.69 ± 3.01	16.2 ± 4.65
$\text{Std}_{A_P=0.00}$	0.120	0.071	0.60	185000	0.00	0.005	0.01 ± 3.01	6.96 ± 4.65
$\text{Std}_{A_P=0.02}$	0.120	0.071	0.60	185000	0.02	0.005	1.03 ± 3.01	6.23 ± 4.65
$\text{Std}_{A_P=0.05}$	0.120	0.071	0.60	185000	0.05	0.005	5.05 ± 3.01	6.42 ± 4.65
$\text{Std}_{N=250k}$	0.120	0.071	0.60	250000	0.01	0.005	0.53 ± 2.59	5.47 ± 4.00
$\text{Std}_{N=1M}$	0.120	0.071	0.60	1000000	0.01	0.005	0.77 ± 1.29	5.86 ± 2.00
$\text{Std}_{N=2M}$	0.120	0.071	0.60	2000000	0.01	0.005	0.77 ± 0.92	6.23 ± 1.41
$\text{Std}_{N=4M}$	0.120	0.071	0.60	4000000	0.01	0.005	0.64 ± 0.65	5.40 ± 1.00

Table 3: Settings used in each scenario with the corresponding A_P and a_{fs} resolution. Scenarios investigated include the physics scenarios mentioned in Section 5.2 and the systematic variation of the input parameters from a "Standard" set based upon the expected $B_s \to D_s^- \mu^+ \nu_\mu$ lifetime resolution.

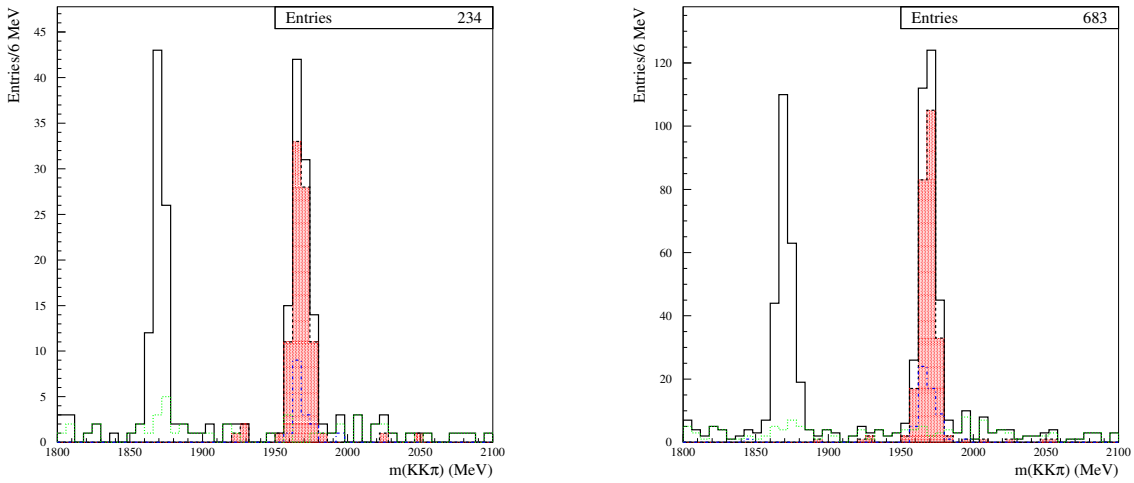

Figure 12: LHCb $D_s^{\pm}\mu^{\mp}$ selection results from recent Monte Carlo studies from [3], reproduced with permission. The invariant mass distribution of $K^+K^-\pi^{\pm}$ in opposite-charge $D_s^{\pm}\mu^{\mp}$ combinations, with 34 million inclusive $b\bar{b}$ events is plotted, where all selection cuts except the D_s mass cut have been applied. Left, with trigger requirement. Right, without trigger requirement. The solid line sums all opposite-charge $D_s^{\pm}\mu^{\mp}$ combinations. The red shaded area covers the Monte Carlo true signals. The dotted green line shows the background combinations with fake D_s . The dash-dotted blue line shows the background combinations with true D_s and here there is an obvious peak in the D_s mass window. The lower mass peak around 1869 MeV corresponds to $D^- \to K^+K^-\pi^-$ decay from $B_d^0 \to D^{\pm}\mu^{\mp}\nu_{\mu}$."

$D_s^{\pm}\mu^{\mp}\nu_{\mu}$ and $B_d^0 \to D^{\pm}\mu^{\mp}\nu_{\mu}$. The recently reported LHCb selection for $B_s^0 \to D_s^{\pm}\mu^{\mp}\nu_{\mu}$ with $D_s^{\pm} \to K^+K^-\pi^{\pm}$ [3] is reproduced in Figure 12. This shows that peaking backgrounds are the main contribution to the background to signal ratio B/S of $\sim$ 0.3. We discuss performing a measurement of $\Delta A^{s,d} = A^s_{fs} - A^d_{fs}$ by a subtraction of the charge-specific asymmetry in $B_s^0 \to D_s^{\pm}(K^+K^-\pi^{\pm})\mu^{\mp}\nu_{\mu}$ and $B_d^0 \to D^{\pm}(K^+K^-\pi^{\pm})\mu^{\mp}\nu_{\mu}$ decays which have the same final states. In contrast to the B_s^0 decay, no dedicated yield study for $B_d^0 \to D^{\pm}(K^+K^-\pi^{\pm})\mu^{\mp}\nu$ has been performed. To estimate the relative yields, we reconstructed $B_s^0 \to D_s^{\pm}(K^+K^-\pi^{\pm})\mu^{\mp}\nu_{\mu}$ and $B_d^0 \to D^{\pm}(K^+K^-\pi^{\pm})\mu^{\mp}\nu_{\mu}$ in the same sample of generic $b\bar{b}$ MC events, using equivalent cuts. For the B_d^0 mode, we found 228 signal and 28 background events; for the B_s^0 mode, we found 240 signal and 82 background events. This indicates that we can expect a similar number of $B_d^0 \to D^{\pm}(K^+K^-\pi^{\pm})\mu^{\mp}\nu_{\mu}$ events as $B_s^0 \to D_s^{\pm}(K^+K^-\pi^{\pm})\mu^{\mp}\nu_{\mu}$, with similar or better signal to background.

The measurement of $\Delta A^{s,d}$ can then be combined with B-factory results on a^d_{fs}, or SM calculations of a^d_{fs} such as [11], to allow a determination of a^s_{fs}. We also briefly cover the extra complications in a time-integrated analysis in Sec. 6.2.

6.1 First-Order Contributions to A_{fs}

For a non-zero charge asymmetry, $\delta_c^q \neq 0$, and production asymmetry $\delta_p^q \neq 0$, and perfect proper time resolution (although our arguments hold for an imperfect time resolution also) we find that the measured untagged time-dependent asymmetry, A_{fs}^q, given in Equation 59 can be simplified to first order in δ^q and a_{fs}^q:

$$A_{fs}^q(t) \approx \frac{a_{fs}^q}{2} - \frac{\delta_c^q}{2} - \left(\frac{a_{fs}^q}{2} + \frac{\delta_p^q}{2}\right) \frac{\cos(\Delta m_q t)}{\cosh(\Delta\Gamma_q t/2)} \tag{77}$$

for a precise measurement of a_{fs}^q terms in higher than first order of $\delta_{c,p}$ should not be ignored. The second-order case is discussed in Section 6.3

Now we allow for the case that background enters our sample. With $N(\text{Bg in } f)$ and $N(\text{Bg in } \bar{f})$ being the number of background events in the final state f and $\bar{f}$, respectively, we define the deviation of the background ratio from unity:

$$\begin{aligned} \delta_b &= \frac{N(\text{Bg in } \bar{f})}{N(\text{Bg in } f)} - 1 \\ (1+\delta_b) &= (1+\delta_c^b)(1+\delta_p^b) \end{aligned} \tag{78}$$

where δ_p^b and δ_c^b represent the deviation from unity of the production and detection ratio in the background, respectively, in analogy to the previously defined δ_p and δ_c for signal.

Including the background effects in the the flavour-specific asymmetry, $A_{fs}^{b,q}(t)$ we find

$$A_{fs}^{b,q}(t) = \left(\frac{S}{S+B}\right)^q A_{fs}^q(t) + \left(\frac{B}{B+S}\right)^q \frac{\delta_b^q}{2} \tag{79}$$

where B/S is the background-to-signal ratio. From Equations 77 and 79 we can see that the major pollutants of the measurement of a_{fs}^q are the charge asymmetry δ_c^q, the production asymmetry δ_p^q and the background asymmetry δ_b.

6.2 Measuring $\Delta A^{s,d}$ in Semileptonic Decays

Equations 77 and 79 show that the time-dependent part has a contribution from the production asymmetry, δ_p^q, which can be separated from the time-independent contributions of the charge asymmetry, δ_c^q, and background asymmetry, δ_b^q. In the $B_s^0 \to D_s^\pm(K^+K^-\pi^\pm)\pi^\mp$ channel the charge asymmetry will be reduced due to the charge-symmetric final state. The analysis presented in section 5.1 will enable simultaneous extraction of flavour-specific asymmetry, a_{fs}^s, and the production asymmetry, δ_p^s. On the other hand, in the semileptonic channels the charge asymmetry is expected to be larger. In addition, this channel has a background peaking in the $D_s^\pm$ mass (Figure 12). This makes this measurement much more challenging. Here we propose a subtraction method using a time-dependent analysis of $B_s^0 \to D_s^\pm \mu^\mp \nu_\mu$ and $B_d^0 \to D^\pm \mu^\mp \nu_\mu$, where the $D_s^\pm$ and $D^\pm$ decays are restricted to the same final state, $D_s^\pm, D^\pm \to K^+K^-\pi^\pm$. We show below that this method removes the contribution from the charge asymmetry, δ_c.

Let us examine the time-independent part of $A_{fs}^{b,q}(t)$ including the factor $[(S)/(S+B)]^q$ which we will call $A_{SL,f}^{b,q}$ (Equation 79). The term $A_{SL,f}^{b,q}$ has no contribution from

the production asymmetry but is dependent on the charge asymmetry, the background asymmetry, and the background to signal ratio B/S:

$$A^{b,q}_{SL,\not{t}} \approx \left(\frac{a^q_{fs}}{2} - \frac{\delta^q_c}{2}\right) + \frac{\delta^q_b}{2}\left(\frac{B}{S}\right)^q \tag{80}$$

LHCb's mass resolution, shown in Figure 12, will enable a clean separation of the $B^0_s \to D^\pm_s \mu^\mp \nu_\mu$ and $B^0_d \to D^\pm \mu^\mp \nu_\mu$ decays in the same final states $D^\pm_s, D^\pm \to K^+K^-\pi^\pm$ [3]. Measuring simultaneously the flavour-specific asymmetry for both $B^0_s \to D^\pm_s(K^+K^-\pi^\pm)\mu^\mp\nu_\mu$ and $B^0_d \to D^\pm(K^+K^-\pi^\pm)\mu^\mp\nu_\mu$ now provides a means of removing the primary error from charge asymmetry. We propose to measure the quantity:

$$\begin{aligned}\Delta A^{s,d} = A^{b,s}_{SL,\not{t}} - A^{b,d}_{SL,\not{t}} &= \frac{\delta^d_c}{2} - \frac{\delta^s_c}{2} + \frac{a^s_{fs}}{2} - \frac{a^d_{fs}}{2} + \frac{\delta^s_b}{2}\left(\frac{B}{S}\right)^s - \frac{\delta^d_b}{2}\left(\frac{B}{S}\right)^d \\ &\approx \frac{a^s_{fs}}{2} - \frac{a^d_{fs}}{2} + \frac{\delta^s_b}{2}\left(\frac{B}{S}\right)^s - \frac{\delta^d_b}{2}\left(\frac{B}{S}\right)^d \end{aligned} \tag{81}$$

The big advantage of using $\Delta A^{s,d}$ as an observable is that the the contribution from the charge asymmetry will effectively be removed. Since the B^0_s and B^0_d meson decay into the same final-state particles, δ^s_c and δ^d_c will cancel.

We also have to take into account the time-dependent part of $\Delta A^{s,d}$. Over a large range of proper time resolutions we may perform an integration of the fast B_s oscillations with negligible effect on $\Delta A^{s,d}$ but the slow B_d oscillations must be correctly taken into account. We plan to verify the proposed analysis method with simulation. This subtraction of the asymmetry in semileptonic B^0_s and B^0_d decays will provide a complimentary method to measuring the time-dependent asymmetry $A^s_{fs}(t)$ in $B^0_s \to D^\pm_s\pi^\mp$. We can combine $\Delta A^{s,d}$ with results for a^d_{fs} from the di-lepton asymmetries measured at the B-factories to extract the flavour-specific asymmetry a^s_{fs} in B^0_s mixing.

By examining Equation 81 one realises that both, the background asymmetries δ^s_b and δ^d_b and the background to signal ratio B/S enter into the measurement of $\Delta A^{s,d}$ in the semileptonic decays $B^0_s \to D^\pm_s\mu^\mp\nu_\mu$ and $B^0_d \to D^\pm\mu^\mp\nu_\mu$, and of $A^s_{fs}(t)$ in the hadronic decay $B^0_s \to D^\pm_s\pi^\mp$, respectively. However, when measuring $A^s_{fs}(t)$ in the hadronic decay $B^0_s \to D^\pm_s(K^+K^-\pi^\pm)\pi^\mp$ we can remove the background by fitting to the mass spectrum or by performing a sideband subtraction which is equivalent to measuring δ^s_b and B/S in the data.

For the semileptonic channels the situation is more challenging as there are backgrounds which peak at the D^+_s and D^+ mass for $B^0_s \to D^\pm_s\mu^\mp\nu_\mu$ and $B^0_d \to D^\pm\mu^\mp\nu_\mu$, respectively. Fitting the mass spectrum will remove the combinatoric background but not these peaking backgrounds. Thus possible asymmetries in these backgrounds and the ratio B/S have to be very well understood so that these will not dominate the precision of a measurement of $a^s_{fs} - a^d_{fs}$ from $\Delta A^{s,d}$. In reference [3] we note that most of the peaking background arises from decays of a B meson into a D^+_s and a $D^0/D^\pm/D^\pm_s$ where the latter decays semileptonically to produce a muon. These events are not flavour-specific and can be treated as background, but careful studies will be required to determine the fraction of the different components in the background. Note also that there will be a small fraction

of $B_d^0 \to D_s^+ \mu^- X$ in the peaking background of of $B_s^0 \to D_s^\pm \mu^\mp \nu_\mu$. It will be important to not only use the $D^+ \to K^+K^-\pi^+$ peak to subtract the asymmetry in $B_d^0 \to D^\pm \mu^\mp \nu_\mu$, but also to fit the sidebands as control samples for cross checks.

In addition the D0 analysis shows that reversing the magnetic field will be imperative for this analysis [19]. This will allow to separate the data sample into several categories. For example dividing the selected events into eight samples, i.e. two magnetic field polarities, two charges of the muon and the sign of muon-momentum in the horizontal (bending) plane (muons going left and right) will allow us to determine the detection and background asymmetries for positive and negative muons simultaneously. The same-charge combinations of $D_s^\pm \mu^\pm$ or $D^\pm \mu^\pm$ can also be used as control sample to study the asymmetry in the background. Ways of measuring the charge asymmetry in muons, pions and kaons are being investigated. One possibility is to use partially reconstructed decays, where we ignore one of the final state particles in the reconstruction and triggering of the decay chain. The reconstruction efficiency for each charge can be measured by counting how often the particle ignored in the reconstruction of the decay is actually found by the track reconstruction, while the total number of partially reconstructed decays provides the normalisation. Channels being studied for this purpose include $B_s^0 \to J/\psi\phi$ and $D^{*+} \to D^0\pi^+$, followed by $D^0 \to K^-\pi^+$.

6.3 Second-Order Contributions to $\Delta A^{s,d}$

We return to the consideration of all systematic effects, considering the second-order corrections in terms of δ_c^q and δ_p^q. As the value of a_{fs}^q within the Standard Model is around the 10^{-4} level, second order terms in the inherent asymmetries are important to the measurement.

Completing our derivation again, including terms of order a_{fs}^q, δ, δ^2, and expanding up to order δ^2, in both the numerator and the denominator of the measured asymmetry we find:

$$A_{SL}^{q\,\prime} = \frac{2a_{fs}^q - \delta_c\left[2+\delta_p^q\right]}{4+2\delta_p^q+\delta_c\left[2+\delta_p^q\right]} - \left(\frac{2a_{fs}^q+\delta_p^q\left[2+\delta_c\right]}{4+2\delta_c+\delta_p^q\left[2+\delta_c\right]}\right)\frac{\cos(\Delta m_q t)}{\cosh(\Delta\Gamma_q t/2)} \tag{82}$$

(c.f. Equation 59) Here we assume that the detection asymmetry for B_s^0 and B_d^0 decaying to the same final state are identical. We then investigate the time-independent part of Equation 82, and perform the subtraction of charge asymmetry in the two channels as before. The first and second order terms in the numerator vanish, producing:

$$\Delta A^{s,d\,\prime} = A_{SL,t}^{s\,\prime} - A_{SL,t}^{d\,\prime} = \left(\frac{2}{(2+\delta_c)^2+2\delta_p^s+2\delta_p^d+\delta_p^s\delta_p^d}\right)\left(a_{fs}^s - a_{fs}^d\right) \tag{83}$$

The terms in the denominator introduce a small bias in the measurement of $a_{fs}^s - a_{fs}^d$ which can be corrected for. This measurement of $\Delta A^{s,d\,\prime}$ is a particularly useful result as there are no contributions from differences in the production asymmetry which are expected in these two channels. Now including background asymmetry terms, to second

order, we find (from Equations 81 and 83):

$$\Delta A^{s,d\,\prime} = \left(\frac{2}{(2+\delta_c)^2 + 2\delta_p^s + 2\delta_p^d + \delta_p^s\delta_p^d}\right)\left(a_{fs}^s - a_{fs}^d\right) + \frac{\delta_b^s}{2}\left(\frac{B}{S}\right)^s - \frac{\delta_b^d}{2}\left(\frac{B}{S}\right)^d \quad (84)$$

Remaining systematic effects not included in Equation 84 will be of order $a_{fs}\cdot\delta$, δ^3 and $\delta_c^s - \delta_c^d$. We will also inherit any uncertainty in our knowledge of the B/S ratios.

Here we summarise that the comparison of the asymmetry measurements in the two channels, $B_s^0 \to D_s^{\pm}(K^+K^-\pi^{\pm})\mu^{\mp}\nu_\mu$ and $B_d^0 \to D^{\pm}(K^+K^-\pi^{\pm})\mu^{\mp}\nu_\mu$, possible at LHCb, provides a systematically much cleaner measurement of $a_{fs}^s - a_{fs}^d$ in semileptonic decays in the realistic environment of the Large Hadron Collider. The measurement of $\Delta A^{s,d}$ can be combined with the measurements in the hadronic mode $B_s^0 \to D_s^{\pm}\pi^{\mp}$ at LHCb and from measurements of a_{fs}^d at the $\Upsilon(4S)$ resonance (B-factories) and the Tevatron to extract hard constraints on the Standard-Model parameters $a_{fs}^{s,d}$ and hence constrain wide avenues of new physics.

7 Conclusions

We investigated the ability of LHCb to perform a measurement of the parameter a_{fs}^s (equivalent to $2\cdot A_{SL}^s$), which parameterises CP violation in $\mathrm{B_s^0}$ mixing. We extract a_{fs}^s from time-dependent, untagged decay-rate asymmetries in decays to semileptonic and hadronic flavour eigenstates, as proposed in [8]. In the expression for the time-dependent asymmetry, acceptance effects due to the LHCb trigger cancel. The measured asymmetry depends on a_{fs}^s itself, the B-production asymmetry A_p and the charge detection asymmetry A_c. Two of these three parameters can be extracted simultaneously, the third needs to be measured externally.

In a Monte Carlo study we performed a simultaneous fit to a_{fs}^s and A_p. We performed fits for zero charge detection asymmetry and a charge detection asymmetry of 2%. In both cases, the value of A_C was kept constant in the fit. Background effects were ignored. We find a statistical precision on a_{fs}^s of $\sim 0.2\%$ for $1M$ events. For $2\,\mathrm{fb}^{-1}$ of LHCb data, this corresponds to $\sigma_{a_{fs}^s} \sim 0.2\%$ in the $\mathrm{B_s^0} \to \mathrm{D_s^-}\mu^+\nu_\mu$ channel, and $\sigma_{a_{fs}^s} \sim 0.5\%$ for $\mathrm{B_s^0} \to \mathrm{D_s^-}\pi^+$. If systematic uncertainties can be controlled at a similar level, this will be a considerable improvement over the expected precision of direct a_{fs} measurements at the Tevatron by the end of Run II.

We found no significant dependence of $\sigma_{a_{fs}^s}$ on the value of A_p, and the result is independent of the time resolution. The precision on the production asymmetry, which is extracted simultaneously, depends strongly on the time resolution. We found an uncertainty on the production asymmetry of $\sigma_{A_p} \sim 0.5\%$ in each mode for $2\,\mathrm{fb}^{-1}$.

Besides the important measurement of a_{fs}^s itself, the measurement of the production asymmetry provides valuable input to many other analyses. Interestingly, the measurement of the production asymmetry with this technique remains possible even without external constraints on the charge detection asymmetry as long as a_{fs}^s is small compared to the required precision on the production asymmetry; then one can extract both A_P and A_C under the assumption that $a_{fs} \approx 0$. Since a_{fs}^s is expected to be tiny, this will provide

sufficient precision for most measurements at LHCb, except of course the measurement of a_{fs} itself which is the main focus of this paper.

In the a_{fs} sensitivity study presented here, the charge detection asymmetry is assumed to be determined elsewhere. In reality, there will be an uncertainty on its value which is likely to be the dominant systematic error for this analysis. To eliminate this systematic error, we propose a measurement of the difference $a^s_{fs} - a^d_{fs}$ using $\mathrm{B^0_s}$ and $\mathrm{B^0_d}$ decays to the same final state, e.g. $\mathrm{B^0_s} \to \mathrm{D^-_s}\mu^+\nu_\mu(\mathrm{D_s} \to \mathrm{KK}\pi)$ and $\mathrm{B^0_d} \to \mathrm{D^-}\mu^+\nu_\mu(\mathrm{D} \to \mathrm{KK}\pi)$. In this measurement, the systematic effects due to the charge detection asymmetry cancel. Since in the Standard Model a^s_{fs} and a^d_{fs} are expected to be of opposite sign, $|a^s_{fs} - a^d_{fs}|$ is likely to be larger than either $|a_{fs}|$ or $|a_{fb}|$ - so, while the systematics cancel, the physics contributions add up. In a real measurement, further systematics will have to be considered, especially those coming from background. As discussed in this note, the measurement of $a^s_{fs} - a^d_{fs}$ can be expected to be more robust against systematic uncertainties stemming from possible CP asymmetries in background, than separate a^s_{fs} and a^d_{fs} measurements.

A Notation

- $|\mathrm{B}^0\rangle$ is a B^0_d or a B^0_s flavour eigenstate.
- $|\overline{\mathrm{B}}^0\rangle$ is a $\overline{\mathrm{B}}_\mathrm{d}$ or a $\overline{\mathrm{B}}_\mathrm{s}$ flavour eigenstate.
- $|B_H\rangle$ and $|B_L\rangle$ are the heavy and light mass eigenstates.
- $|\mathrm{B}^0(t)\rangle$ is an evolving, oscillating B-meson that was a $|\mathrm{B}^0\rangle$ at $t = 0$.
- $|\overline{\mathrm{B}}^0(t)\rangle$ is an evolving, oscillating B-meson that was a $|\overline{\mathrm{B}}^0\rangle$ at $t = 0$.
- f a final state the B meson decays to, $\bar{f}$ is its CP-conjugate.
- A_f is the decay amplitude of a B^0 flavour eigenstate to f, $A_f = \langle f|H_I|\mathrm{B}^0\rangle$, where H_I represents the interaction Hamiltonian
- $\bar{A}_f$ is the decay amplitude of a $\overline{\mathrm{B}}^0$ flavour eigenstate to f, $\bar{A}_f = \langle f|H_I|\overline{\mathrm{B}}^0\rangle$.
- Similarly, $A_{\bar{f}} = \langle \bar{f}|H_I|\mathrm{B}^0\rangle$, $\bar{A}_{\bar{f}} = \langle \bar{f}|H_I|\overline{\mathrm{B}}^0\rangle$
- N_f is a normalisation factor which is the same for all decay rates.

B Finite Time resolution

To obtain the measured decay rates with finite time resolution we need to calculate:

$$\Gamma_i \;=\; f_i(a_{fs}) \int_0^\infty e^{-\Gamma\, t'} \left(\cosh\left(\frac{1}{2}\Delta\Gamma\, t'\right) \pm \cos\left(\Delta m\, t'\right)\right) \frac{1}{\sqrt{2\pi}\sigma} e^{\frac{(t'-t)^2}{2\sigma^2}} dt' \qquad (85)$$

This can be expressed as

$$\begin{aligned}\Gamma_i(t) \;&=\; f_i(a_{fs})\mathsf{Re}\left\{\frac{1}{\sqrt{2\pi}\sigma}\int_0^\infty e^{-\Gamma\, t'}\left(\frac{1}{2}e^{\frac{1}{2}\Delta\Gamma\, t'} + \frac{1}{2}e^{-\frac{1}{2}\Delta\Gamma\, t'} \pm e^{i\Delta m\, t'}\right) e^{\frac{(t'-t)^2}{2\sigma^2}} dt'\right\} \\ &=\; f_i(a_{fs})\mathsf{Re}\left\{\frac{1}{\sqrt{2\pi}\sigma}\int_0^\infty \left(\frac{1}{2}e^{-\left(\Gamma-\frac{1}{2}\Delta\Gamma\right)t'} + \frac{1}{2}e^{-\left(\Gamma+\frac{1}{2}\Delta\Gamma\right)t'} \pm e^{-(\Gamma-i\Delta m)\,t'}\right) e^{\frac{(t'-t)^2}{2\sigma^2}} dt'\right\}\end{aligned} \qquad (86)$$

Hence the problem reduces to calculating

$$\frac{1}{\sqrt{2\pi}\sigma}\int_0^\infty e^{-A\, t'} e^{-\frac{(t'-t)^2}{2\sigma^2}}\, dt' \qquad (87)$$

for different (sometimes complex) values of A. This can be re-written as:

$$\frac{1}{\sqrt{2\pi}\sigma} e^{-A\,t+\frac{1}{2}A^2\sigma^2} \int_0^\infty e^{-\frac{1}{2\sigma^2}\left(t'-\left(t-\sigma^2\,A\right)\right)^2}\,dt' \tag{88}$$

Changing the integration variable to $x \equiv \frac{t'}{\sigma}$:

$$\frac{1}{\sqrt{2\pi}\sigma} \int_0^\infty e^{-\frac{1}{2\sigma^2}\left(t'-\left(t-\sigma^2\,A\right)\right)^2}\,dt' = \frac{1}{\sqrt{2\pi}} \int_0^\infty e^{-\frac{1}{2}\left(x-\left(\frac{t}{\sigma}-\sigma\,A\right)\right)^2}\,dx = \frac{1}{\sqrt{2\pi}} \int_{-\infty+\left(\frac{t}{\sigma}-\sigma\,A\right)}^{\left(\frac{t}{\sigma}-\sigma\,A\right)} e^{-\frac{1}{2}x^2}\,dx$$

For real A:

$$\frac{1}{\sqrt{2\pi}} \int_{-\infty+\left(\frac{t}{\sigma}-\sigma\,A\right)}^{+\left(\frac{t}{\sigma}-\sigma\,A\right)} e^{-\frac{1}{2}x^2}\,dx = \frac{1}{\sqrt{2\pi}} \int_{-\infty}^{\left(\frac{t}{\sigma}-\sigma\,A\right)} e^{-\frac{1}{2}x^2}\,dx = \text{Freq}\left(\frac{t}{\sigma}-\sigma\,A\right) \tag{89}$$

where Freq is the frequency function, defined by

$$\text{Freq}(y) \equiv \frac{1}{\sqrt{2\pi}} \int_{-\infty}^{y} e^{-\frac{1}{2}x^2}\,dx \tag{90}$$

the Cernlib implementation of this function is available in root as `TMath::Freq`. The frequency function is related to the more familiar error function by

$$F(y) = \frac{1}{2} + \frac{1}{2}\text{erf}\left(\frac{y}{\sqrt{2}}\right) \tag{91}$$

which can also be found in root.

For complex $A = \Gamma - i\Delta m$ we find

$$\frac{1}{\sqrt{2\pi}} \int_{-\infty+\left(\frac{t}{\sigma}-\sigma\,A\right)}^{\left(\frac{t}{\sigma}-\sigma\,A\right)} e^{-\frac{1}{2}x^2}\,dx = -i\frac{1}{2}\text{erfi}\left(\frac{\Delta m\sigma + i\left(\frac{t}{\sigma}-\sigma\Gamma\right)}{\sqrt{2}}\right) + \frac{1}{2} \tag{92}$$

where erfi is the imaginary error function defined by:

$$\text{erfi}(z) = -i\text{erf}(-iz) \tag{93}$$

This is related to the complex error function:

$$w(z) = e^{-z^2}\left(1 - i\text{erfi}(iz)\right) \tag{94}$$

which is implemented in root as `TMath::FastComplexErrFunc`, which returns a complex data type, or `TMath::FastComplexErrFuncRe` and `TMath::FastComplexErrFuncIm` which return doubles. With this, Equation 85 becomes:

$$\begin{aligned}
&\int_0^\infty e^{-\Gamma t'}\left(\cosh\left(\frac{1}{2}\Delta\Gamma\, t'\right)\pm\cos\left(\Delta m\, t'\right)\right)\frac{1}{\sqrt{2\pi}\sigma}e^{\frac{(t'-t)^2}{2\sigma^2}}dt' = \\
&\quad \frac{1}{2}\exp\left(-\left(\Gamma-\frac{1}{2}\Delta\Gamma\right)t+\frac{1}{2}\sigma^2\left(\Gamma-\frac{1}{2}\Delta\Gamma\right)^2\right)\mathrm{Freq}\left(\frac{t}{\sigma}-\sigma\left(\Gamma-\frac{1}{2}\Delta\Gamma\right)\right) \\
&+\quad \frac{1}{2}\exp\left(-\left(\Gamma+\frac{1}{2}\Delta\Gamma\right)t+\frac{1}{2}\sigma^2\left(\Gamma+\frac{1}{2}\Delta\Gamma\right)^2\right)\mathrm{Freq}\left(\frac{t}{\sigma}-\sigma\left(\Gamma+\frac{1}{2}\Delta\Gamma\right)\right) \\
&\pm\quad \mathsf{Re}\Bigg\{\exp\left(-\Gamma t+\frac{1}{2}\sigma^2\Gamma^2-\frac{1}{2}\Delta m^2\sigma^2\right)\exp\left(i\Delta m\left(t-\Gamma\sigma^2\right)\right) \\
&\quad \times\left(\frac{1}{2}-i\frac{1}{2}\mathrm{erfi}\left(\frac{\Delta m\sigma+i\left(\frac{t}{\sigma}-\sigma\Gamma\right)}{\sqrt{2}}\right)\right)\Bigg\}
\end{aligned} \tag{95}$$

Taking out common factors:

$$\begin{aligned}
&\int_0^\infty e^{-\Gamma t'}\left(\cosh\left(\frac{1}{2}\Delta\Gamma\, t'\right)\pm\cos\left(\Delta m\, t'\right)\right)\frac{1}{\sqrt{2\pi}\sigma}e^{\frac{(t'-t)^2}{2\sigma^2}}dt' = \\
&\quad e^{-\Gamma t}\, e^{\frac{1}{2}\Gamma^2\sigma^2}\Bigg[e^{\frac{1}{8}\sigma^2(\Delta\Gamma)^2}\Bigg\{ \\
&\quad \frac{1}{2}\,e^{\frac{1}{2}\Delta\Gamma\left(t-\sigma^2\Gamma\right)}\mathrm{Freq}\left(\frac{t}{\sigma}-\sigma\left(\Gamma-\frac{1}{2}\Delta\Gamma\right)\right) \\
&+\quad \frac{1}{2}\,e^{-\frac{1}{2}\Delta\Gamma\left(t-\sigma^2\Gamma\right)}\mathrm{Freq}\left(\frac{t}{\sigma}-\sigma\left(\Gamma+\frac{1}{2}\Delta\Gamma\right)\right)\Bigg\} \\
&\pm\quad e^{-\frac{1}{2}\Delta m^2\sigma^2}\mathsf{Re}\Bigg\{e^{i\Delta m\left(t-\Gamma\sigma^2\right)} \\
&\quad \times\left(\frac{1}{2}-i\frac{1}{2}\mathrm{erfi}\left(\frac{\Delta m\sigma+i\left(\frac{t}{\sigma}-\sigma\Gamma\right)}{\sqrt{2}}\right)\right)\Bigg\}\Bigg]
\end{aligned} \tag{96}$$

The expression simplifies significantly if we assume that $t \gg \sigma$, because then the Freq terms tend towards 1 and erfi towards i.

$$\begin{aligned}
&\int_0^\infty e^{-\Gamma t'}\left(\cosh\left(\frac{1}{2}\Delta\Gamma\, t'\right)\pm\cos\left(\Delta m\, t'\right)\right)\frac{1}{\sqrt{2\pi}\sigma}e^{\frac{(t'-t)^2}{2\sigma^2}}dt' = \\
&\quad e^{-\Gamma t}\, e^{\frac{1}{2}\Gamma^2\sigma^2}\left[e^{\frac{1}{8}\sigma^2(\Delta\Gamma)^2}\cosh\left(\frac{1}{2}\Delta\Gamma\,\left(t-\sigma^2\Gamma\right)\right)\pm e^{-\frac{1}{2}\Delta m^2\sigma^2}\cos\left(\Delta m\left(t-\Gamma\sigma^2\right)\right)\right]
\end{aligned} \tag{97}$$

References

[1] Z. Ligeti *et al.*, [arXiv:hep-ph/0604112] (2006).

[2] U. Nierste, [arXiv:hep-ph/0406300] (2006).

[3] O. Leroy *et al.*, LHCb note 2007-029.

[4] J. Borel *et al.*, LHCb note 2007-017.

[5] B. Aubert *et. al*, the BaBar collaboration, [arXiv:hep-ex/0202041] (2002).

[6] E. Nakano *et al.* [Belle Collaboration], Phys. Rev. D **73** (2006) 112002 [arXiv:hep-ex/0505017].

[7] K. Anikeev *et al.*, FERMILAB-Pub-01/197, [arXiv:hep-ph/0201071].

[8] I. Dunietz, R. Fleischer and U. Nierste, Phys. Rev. D **63** (2001) 114015 [arXiv:hep-ph/0012219].

[9] O. Schneider, for the Particle Data Group, in [22], pp. 836-842 (2006).

[10] S. Laplace, Z. Ligeti, Y. Nir and G. Perez, [arXiv:hep-ph/0202010] (2002).

[11] A. Lenz, U. Nierste, [arXiv:hep-ph/0612167] (2006).

[12] M. Beneke, G. Buchalla, A. Lenz and U. Nierste, [arXiv:hep-ph/0307344] (2003).

[13] C. S. Kim, J. Lee, W. Namgung, Phys. Rev. D **59** (2003) pp. 114006-1 – 114006-7.

[14] C. S. Kim, J. Lee, W. Namgung, Phys. Rev. D **59** (2003) pp. 114005-1 – 114005-11.

[15] Y. Grossman, Y. Nir and G. Raz, Phys. Rev. Lett. **97** (2006) 151801 [arXiv:hep-ph/0605028].

[16] A. Abulencia *et. al*, the CDF collaboration, Phys. Rev. Lett. **97** (2006) pp. 062003-1 – 062003-7.

[17] E. Norrbin and T. Sjostrand, Eur. Phys. J. C **17** (2000) 137 [arXiv:hep-ph/0005110].

[18] D. E. Jaffe *et al.* [CLEO Collaboration], Phys. Rev. Lett. **86** (2001) 5000 [arXiv:hep-ex/0101006].

[19] V. M. Abazov *et al.* [D0 Collaboration], Phys. Rev. D **74** (2006) 092001 [arXiv:hep-ex/0609014].

[20] T. Aaltonen *et al.* [CDF Collaboration], (2007)

[21] E. Barberio *et. al*, the Heavy Flavor Averaging Group, [arXiv:hep-ex/0603003] (2006).

[22] W.-M. Yao et al. *et. al*, the Particle Data Group, Journal of Physics G 33, 1 (2006) pp. 1-1232.

[23] V. M. Abazov *et al.* [D0 Collaboration], [arXiv:hep-ex/0702030].

[24] V. M. Abazov *et al.* [D0 Collaboration], Phys. Rev. Lett. **98** (2007) 151801 [arXiv:hep-ex/0701007].